New Insights into the Structural and Stratigraphic Evolution of the Malay Basin Using 3D Seismic Data: Implications for Regional Carbon Capture and Storage Potential

Iain de Jonge-Anderson*[1], Ana Widyanita[1,2], Andreas Busch[1], Florian Doster[1], Uisdean Nicholson[1]

[1]Institute of GeoEnergy Engineering (IGE), School of Energy, Geoscience, Infrastructure & Society, Heriot-Watt University, Edinburgh, EH14 4AS, UK

[2]PETRONAS Research Sdn. Bhd., Malaysia

*Corresponding author (email: i.anderson@hw.ac.uk, X: @iaindja)

ORCiD: 0000-0002-9438-8194 (IdJ-A)

New Insights into the Structural and Stratigraphic Evolution of the Malay Basin Using 3D Seismic Data: Implications for Regional Carbon Capture and Storage Potential

Iain de Jonge-Anderson*[1], Ana Widyanita[1,2], Andreas Busch[1], Florian Doster[1], Uisdean Nicholson[1]

[1]Institute of GeoEnergy Engineering (IGE), School of Energy, Geoscience, Infrastructure & Society, Heriot-Watt University, Edinburgh, EH14 4AS, UK

[2]PETRONAS Research Sdn. Bhd., Malaysia

*Corresponding author (email: i.anderson@hw.ac.uk)

ORCiD: 0000-0002-9438-8194 (IdJ-A)

Acknowledgements

Abstract

The Malay Basin is a mature hydrocarbon province that is being re-assessed for CO_2 storage. Selecting appropriate storage sites requires a comprehensive understanding of the structural and stratigraphic history of the basin, but previous studies of the basin have been limited to observations from either regional, 2D seismic lines or individual 3D seismic volumes. Here, we access and utilize a basin-wide (~40,000 km^2) 3D seismic and well database to describe the structural and stratigraphic features of the basin, particularly those within the uppermost ~ 4 km (Oligocene to Recent), to gain new insights into the evolution of the basin. E-W transtensional rift basins first developed because of sinistral shear across a NW-SE strike-slip zone. The NW-SE basin morphology seen today was generated during the late Oligocene – early Miocene during which time dextral motion across marginal hinge zones created en-echelon antithetic, extensional faults and pull-apart basins, especially well preserved along the western margin of the basin. Collisional forces to the southeast during the early-middle Miocene resulted in shallowing of the basin, intermittent connection to the South China Sea and a cyclic depositional pattern during the Miocene. During the late Miocene, significant uplift of the basin resulted in a major unconformity with up to 4 km of erosion and exhumation in the southeast of the basin. In the centre and northwest region, the inversion of deeper E-W rifts resulted in the folding of Miocene sequences, and the formation of large anticlines parallel to the rift-bounding faults. The Pliocene-Pleistocene history is more tectonically quiescent, but some extensional faulting continued to affect the northwest part of the basin. Larger glacio-eustatic sea-level fluctuations during this time resulted in major changes in sedimentation and

erosion on the Sunda Shelf, including the formation of a middle-Pliocene unconformity. These structural events have created a variety of hydrocarbon traps across the basin, of different ages, including transpressional anticlines, rollover anticlines and tilted fault blocks. Each of these has discrete and distinct trap elements, with important implications for their CO_2 storage potential.

1. Introduction

The geodynamic history of Sundaland and the structural evolution of Cenozoic rift basins located on it have been the subject of many scientific studies in the past. The evolution of these basins is influenced by various important regional geological events, including the Himalayan collision, the opening of the South China Sea and subduction/collision along various plate boundaries (Doust & Sumner, 2007; Hall & Morley, 2004; Hall et al., 2009; Metcalfe, 2011, 2017; Morley, 2002; Pubellier & Morley, 2014). Despite this increase in our understanding of the tectonic boundary conditions at the plate-level, a detailed understanding of the evolution of these basins is limited. This is despite the fact that many of these basins have been extensively explored for hydrocarbons, resulting in vast geophysical and geological datasets associated with drilling.

The largest of these basins is the Malay Basin, which is around 500 km long and 200 km wide and strikes NW-SE, roughly parallel with the Malay Peninsula (Fig. 1B). It lies in coastal waters less than 100 km from the Malaysian shoreline, but its northwest, northeast and southeast margins extend into waters belonging to Thailand, Vietnam, and Indonesia respectively. It is bound by basement highs to the southwest (Terengganu Shelf) and northeast (Khorat Swell) that eventually rise to crop out onshore, where they form the Malay Peninsula and Vietnamese/Cambodian coast of the Southeast Asian landmass, respectively. To the northwest, it is separated from the Pattani Basin by the Narawathi High. To the southeast, it is separated from the Penyu and West Natuna Basins by the Tenggol High and the southern promontory of the Khorat Swell, respectively.

The Malay Basin is a prolific petroleum basin (Madon, 2021; Rice-Oxley & Abu-Bakar, 2022), hosting over 181 discoveries, and over 14.8 billion barrels of oil equivalent (bboe) recoverable resources (Madon, 2021). Therefore, most scientific understanding of its stratigraphy and structure comes from activities associated with the exploration, appraisal, and development of hydrocarbon resources. Early stratigraphic frameworks for the basin were published by Woolands & Haw (1976) Armitage & Viotti (1977), Ramli (1988) and Yakzan et al (1996), all of which describe the different schemes adopted by the various companies that have explored the region. Early insights into the structure of

the basin were published by Kuang (1988) and Ng (1987) but the first detailed accounts were published in studies reporting on seismic data analysis during the mid-late 1990s. These accounts initially focused on the evidence for strike-slip deformation and structural inversion within the basin, particularly along its western flank (Tjia, 1994; Tjia and Liew, 1996, Liew, 1994). These were followed by a series of publications that defined the basin's broader structural framework and kinematic history through integrating seismic, gravity and magnetic datasets (Liew, 1997; Ngah et al (1996); Madon, 1997, Madon & Watts, 1998).

More recently, scientific focus has shifted to understanding the petroleum system (Bishop, 2002; Doust & Sumner, 2007; Doust, 2017; Madon et al., 2006; Nayak et al., 2023; Petersen et al., 2011), overpressure (Ahmed Satti et al., 2016; Madon, 2007; Tingay et al., 2011, 2013), subtle stratigraphic and structural features at either the field-scale (Almasgari et al., 2020; Babkir et al., 2022; Hou et al., 2008) or the regional-scale (Alqahtani et al., 2015, 2017; Miall, 2002) and the emerging basement hydrocarbon play (Madon et al., 2020). The only recent regional reassessment of the geological structure is that of Mansor et al. (2014), who used insights from the interpretation of deep (8 s TWT) regional 2D lines to describe the basement structure and fault patterns.

The Malay Basin is also considered to be an important area for the future geological storage of CO_2 (Abd Rahman et al., 2022; Hasbollah et al., 2020), however, these studies employ relatively broad evaluations of subsurface geology in their analyses. The Malay Basin contains numerous mature fields that could be re-purposed for Carbon Capture and Storage (CCS), and these offer an abundance of data and production history, but their potential is hindered by limited storage capacity, field availability and pressure changes following depletion. There is currently insufficient capacity within Malay Basin depleted fields to meet CO2 storage requirements, hence it is important to study and mature other storage site types, one of which is saline aquifers. However, there is often significantly less information available for saline aquifers, particularly regarding reservoir/caprock distribution and the presence of structural traps.

This study was motivated by the need to better understand the distribution of potential CCS traps and their associated risks across the Malay Basin. To do this, a comprehensive evaluation of the basin's structure and stratigraphy was undertaken. The aims of this were to achieve a better understanding of geological events affecting the basin (and wider SE Asia region) and determine the timing of CCS trap formation and their present-day spatial distribution. Key to this was the interpretation of an extensive 3D seismic database that has not been utilised in previous studies of the basin.

2. Geological Setting

2.1. Structural Setting

The basin lies on the Sunda Shelf; a region of shallow water (< 100 m) that is located between Mainland Southeast Asia, the Malay Peninsula, and the large islands of Sumatra, Java, and Borneo (Fig. 1A, B). The shelf has undergone multiple cycles of emergence and submergence since 400 ka (McGrath et al., 2023), and while emergent, created in an extensive, linked biogeographical and geological system across Southeast Asia, referred to as Sundaland. The continental core of Sundaland, the Sunda Plate, was assembled during the Mesozoic and is the result of the closure of multiple Tethyan oceans and the amalgamation of continental fragments derived from the India-Australian margin of eastern Gondwana (Hall and Morley, 2004; Hall et al., 2009; Metcalfe, 2009, 2011; Morley, 2012). To the west, south, and east, the plate is bounded by complex and tectonically active regions, following subduction of the Indian, Australian and Philippine Sea plates respectively. By contrast, the plate's northern margin is more tectonically quiescent following slow convergence with the Eurasian and Yangtze plates.
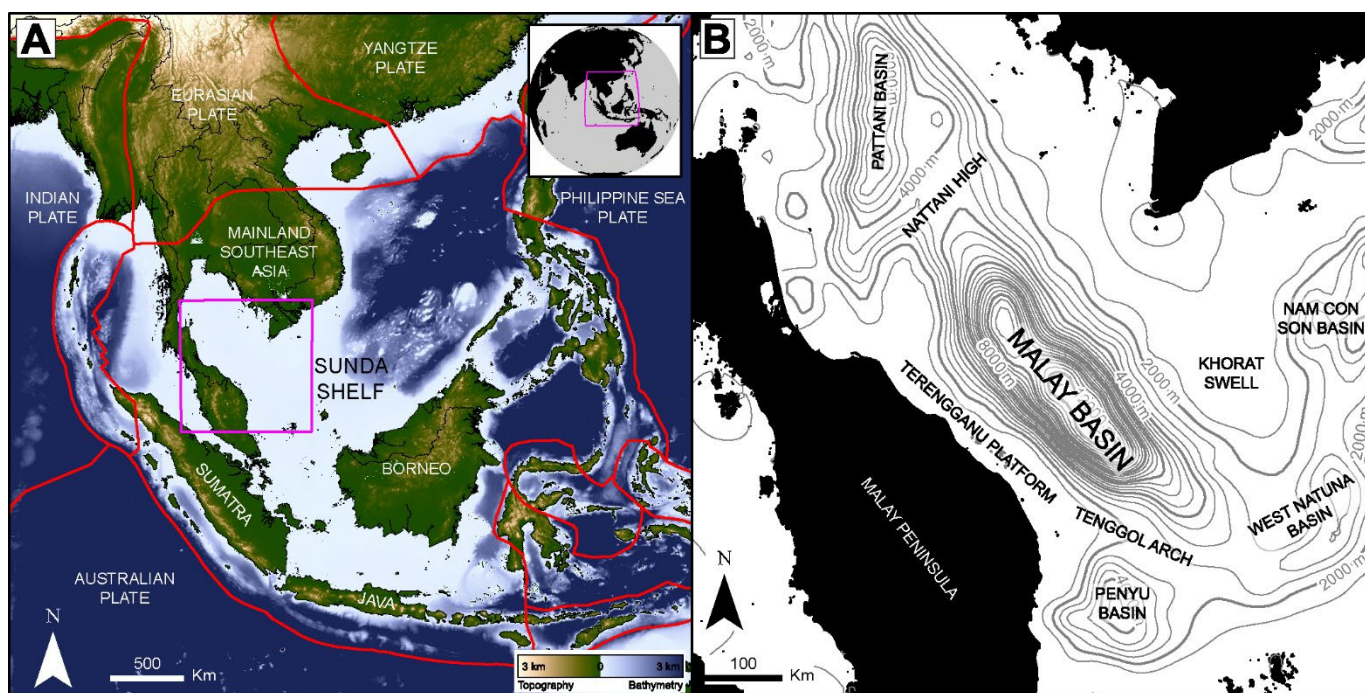

Figure 1: (A) Map of Southeast Asia highlighting bathymetry and topography (GEBCO, 2023) and plate boundaries (Bird, 2003; Argus et al., 2011). (B) Map of the waters between the Malay Peninsula and Mainland Southeast Asia highlighting the total sediment thickness (Straume et al., 2019) and locations of major basins and highs.

The Malay Basin is one of several continental rift basins that lie on the west of Sundaland extending from the Gulf of Thailand down to the Natuna Islands (Fig. 1B). Extension across the area now occupied by the Malay Basin started during the late Eocene (Hall & Morley, 2004; Madon, 1997; Pubellier & Morley, 2014; Tjia, 1998) generating a pattern of E-W-striking faults and narrow basins (Fig. 2) (Tjia, 2014; Tjia and Liew, 1996). This structural fabric was produced in

103   a transtensional regime, involving extension across a broadly NW-SE left-lateral (sinistral) shear zone, generally believed

104   to be the southerly and offshore continuation of Three Pagodas and Mae Ping fault zones (Doust and Sumner, 2007;

105   Fyhn et al., 2010; Madon, 1997; Manshor et al., 2014). This strike-slip zone was active since the latest Eocene following

106   the lateral extrusion of continental blocks following collision of the Indian and Asian continents (Molnar & Tapponnier,

107   1975; Pubellier & Morley, 2014; Tapponier et al., 1982).

108   The Malay Basin continued to open during the Oligocene, with dextral movement along basin-margin hinge zones (e.g.,

109   Western Hinge Fault Zone (WHFZ) (Tjia, 1994)). These hinge zones strike NW-SE and their development has been linked

110   to either the Three Pagodas fault zone, or rollback associated with subduction rollback of the Indian plate oceanic crust

111   (Morley; 2002; Pubellier & Morley, 2014). Lateral motions across these faults initially created small pull-apart basins

112   along the hinge zones that would be the loci for pre-late Oligocene sediments, before the basin widened and opened

113   fully (Tjia, 1994). Continued shearing produced roughly NW-SE-striking faults that linked both hinge zones and created

114   a fabric of NNW-SSE-striking sub-basins and highs within the basin (Manshor et al., 2014).
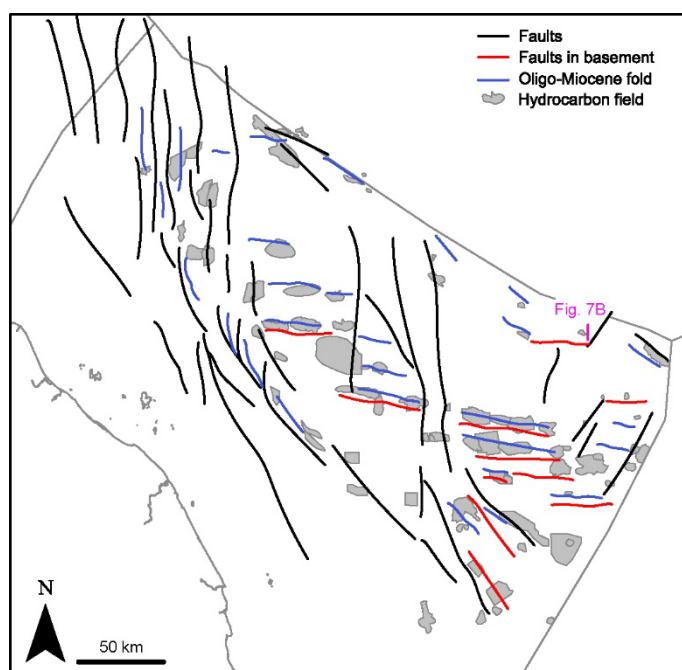
115

116   *Figure 2: Major structures in the Malay Basin (after Tjia & Liew, 1996)*

117   Miocene compression caused the uplift and inversion of many Sundaland rift basins, particularly those located along

118   its southern margin (Doust & Sumner, 2007; Pubellier & Morley, 2014). Inversion structures associated with these uplift

119   events have been well-documented in the West Natuna Basin. Here, several small unconformities have been noted

120   within the early-middle Miocene, with a more prominent, basin-wide unconformity removing most of the upper-

121   middle Miocene and lower-upper Miocene (Ginger et al., 1993). This middle-late Miocene unconformity is believed to

122   be linked to the halting of spreading in the South China Sea, the westward push of the Pacific plate, the subduction of

123   the Sulu Sea and the collision of the Australian plate (Morley et al., 2003; Tjia, 1998).

124   In the Malay Basin, a prominent late Miocene (Tortonian) unconformity referred to as the "Intra-Late Miocene

125   Unconformity" (Ramli, 1988) or the "Upper Miocene Unconformity" (Yakzan et al., 1996) extends across the entire

126   basin. This is equivalent to the middle-late Miocene unconformity described above within the West Natuna Basin and

127   formed following the reversal in slip sense along the NW-SE strike-slip faults, and structural inversion of many of the

128   pre-existing W-E depocentres (Tjia, 1998).

129   A smaller, "Top Middle Miocene Unconformity" also exists, where the lower part of Group E is missing at the southeast

130   part of the basin (Yakzan et al., 1996). This has been attributed to a major relative sea-level fall across the area (Yakzan

131   et al., 1996). This unconformity is difficult to identify in the Malay Basin, particularly as it was subsequently overprinted

132   by the intra-late Miocene unconformity over much of the basin. However, early Miocene unconformities have been

133   described within the West Natuna Basin (Ginger et al., 1996), often ascribed to compressional stresses that resulted

134   from the collision of various fragments of the Australian plate against the southeast margin of Sundaland (Doust &

135   Sumner, 2007; Morley et al., 2003; Pubellier and Morley, 2014).

136   The Malay Basin, and the wider region, experienced little tectonic activity during the Pliocene and Pleistocene. The

137   Pattani Basin, in the north, was not affected by late Miocene inversion and, instead, has been steadily subsiding since

138   the early Miocene (Bustin & Chonchalawit, 1995). In the southeast, following significant structural inversion, the West

139   Natuna Basin experienced a renewed phase of subsidence (Ginger et al., 1993), which has tentatively been linked to

140   the termination of the rotation of Borneo (Morley et al., 2003).

141   ## 2.2. Stratigraphy

142   There are several stratigraphic nomenclatures used to describe the Cenozoic sediments within the Malay Basin

143   (Armitage & Viotti, 1977; Ramli, 1988; Woollands & Haw, 1976; Yakzan et al., 1996), however, the main subdivisions

144   are fundamentally the same (Fig. 3). The first basin-wide scheme was proposed by Esso, in which "Groups" are given

145   alphabetical notation (A-M) based on seismic characteristics (Madon, 1999b), though this was subsequently adjusted

146   following on a revised biostratigraphy for the basin (Yakzan et al., 1996). This notation is the most frequently used

147   scheme within the basin and is adopted for this study, though other schemes are presented in Figure 3 for reference.

148 While the oldest sediments drilled within the basin are Oligocene in age, seismic and biostratigraphic observations

149 from adjacent areas imply an older, middle-late Eocene age date for formation of the basin (Fyhn et al., 2010; Kessler

150 et al., 2020). Since this initial opening, over 14 km of sediments are estimated to have been deposited in the centre of

151 the basin (Arshad et al., 1995). Because of the thick sedimentary cover, the current understanding of the oldest

152 sediments is almost exclusively from the southeast flank of the basin, where structural inversion and limited post-rift

153 subsidence have resulted in these sediments being at depths still feasible for drilling (3-4 km). These sediments belong

154 to the Oligocene (Rupelian to Chattanian) Groups M and L, equivalent to the Ledang and Seligi formations (Fig. 3). Both

155 groups consist of fining-upwards packages, consisting of basal sandstones capped by a thick shale (Yakzan et al., 1996).

156 The shale at the top of Group M (Ledang Shale) was deposited in freshwater lacustrine conditions (Yakzan et al., 1996),

157 however, there is debate about the depositional environment of Group L (Seligi Shale). Some authors note the presence

158 of marine foraminifera (Armitage & Viotti, 1977; Yazkan et al., 1996), but Lunt (2021), suggested these were likely caved

159 samples and that nonmarine conditions persisted throughout Group L. The sandstones belonging to each were

160 deposited in an alluvial fan environment by braided fluvial systems and distributary mouthbars (Jumari et al., 2011;
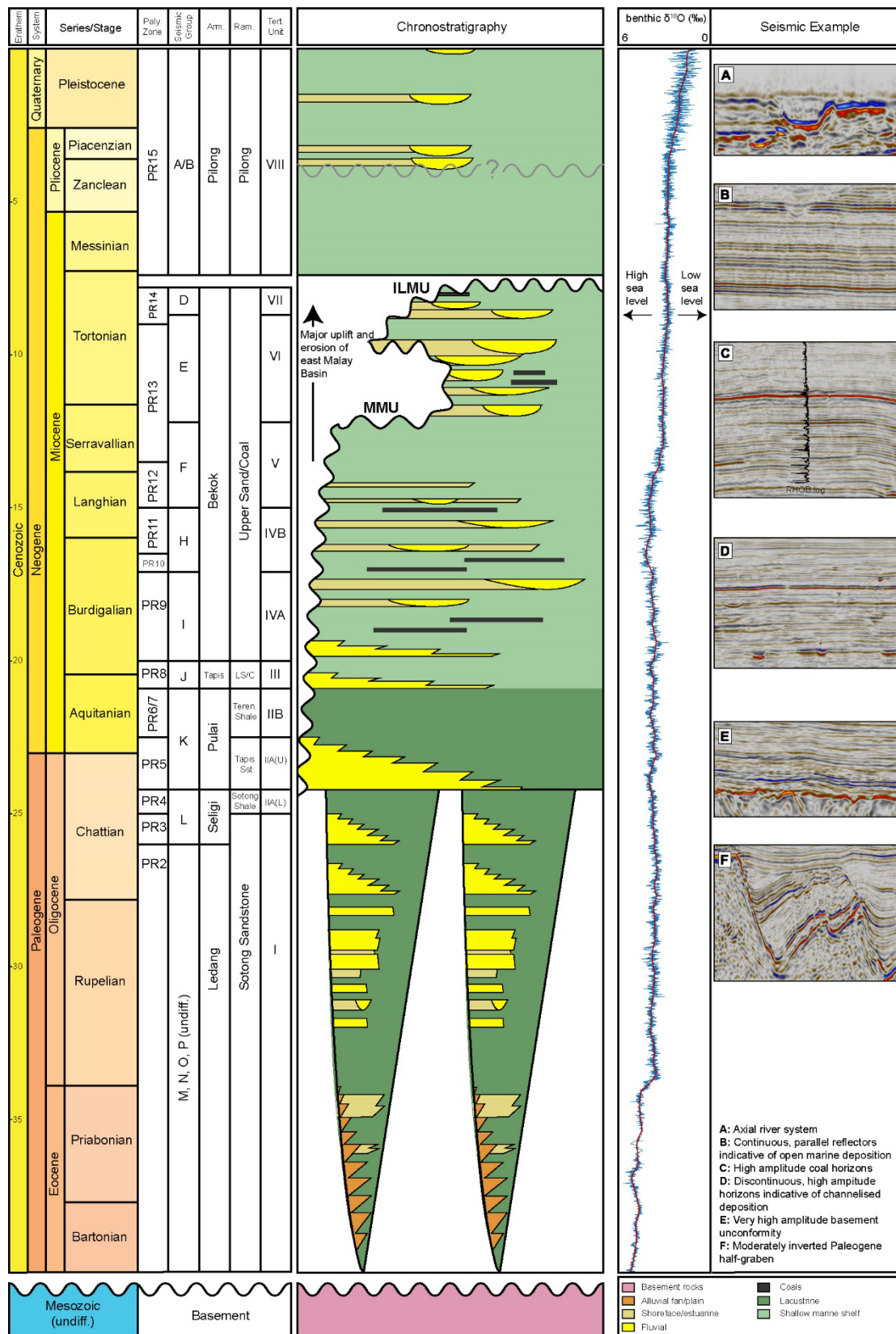
161 Rosly et al., 2019; Yusak, 2012).

Figure 3: Stratigraphic chart for the Malay Basin (after Armitage & Viotti, 1977; Lunt, 2021; Madon, 1999a, b; Manshor et al., 2014; Ramli, 1988; Yakzan et al., 1996). Oxygen isotope data is after Westerhold et al. (2020).

The upper Oligocene (Chattanian) to lower Miocene (Aquitanian) Group K has been drilled extensively along the basin margins but also in more central, inverted areas. It is characterised by a fining-upward package consisting mainly of braided fluvial/deltaic sandstones in the lower part and a thick shale in the upper part. The upper shale ("K Shale") is

169   an important unit in which palynological indicators suggest a transition from land-locked lacustrine deposition to

170   nearshore freshwater swamps (Lunt, 2021), with increasingly brackish waters (Armitage & Viotti, 1977).

171   A shift in tectonic regime from rifting to thermal subsidence occurred at the start of the Miocene during which time

172   the basin also experienced its first marine incursion (Yakzan et al., 1996). The basin lay at or near sea level with much

173   of the area covered by a lower coastal plain, with fluvio-deltaic systems draining basement highs to the southwest

174   (nearshore Peninsular Malaysia) and northeast (Khorat Swell) (Madon, 1999a; Ramli, 1988). Groups J and I were

175   deposited during the early Miocene (Aquitanian to Burdigalian) within mainly a brackish to shallow marine setting

176   (Shing, 1992).

177   These intervals are important commercially, forming reservoirs in many oil and gas fields and as a result, several core

178   studies have been undertaken. These recognise distinct depositional facies including tidally reworked subtidal bars,

179   estuarine channel sands, storm-related sheet flood sandstones and offshore marine shales (Madon, 1999b; Ramli,

180   1998; Thye, 1996). During this period, the emerging West Natuna block intermittently created a sill that restricted

181   marine waters from entering the Malay Basin from the east. This effect, superimposed on sea level fluctuations,

182   resulted in a Miocene sequence composed of various transgressive-regressive periods and cyclic deposition (Madon,

183   2011; Jirin et al., 2013).

184   The middle Miocene Group F is composed almost entirely of mudstone, with a minor, middle sandstone unit (Yakzan

185   et al., 1996). It also forms a pressure seal across the centre of the basin, with significant overpressure below (Madon,

186   2007). The lower part of this unit corresponds with a period of high regional sea level (Fig. 3).

187   The top of Group F is marked by an unconformity that has removed part of Group E from the southeast of the Malay

188   Basin (Fig. 3). A sea-level fall during the middle-upper Miocene resulted in a basin-wide regression, and the

189   development of a major, southerly-flowing fluvial/delta system along the axis of the basin (Madon, 1994); a marked

190   contrast with the transverse depositional framework present through the early-middle Miocene. The result was the

191   deposition of a thick sequence of coastal plain to shoreface sediments in the lower part of Group E, which are overlain

192   by a marine mudstone (Yakzan et al., 1996).

193   The Pliocene to Recent section of the Malay Basin has been less intensively studied, in part, because it is only a very

194   minor reservoir interval for hydrocarbons (Madon, 2021). Early accounts of the stratigraphy describe an entirely marine

195   section, consisting mainly of mudstone with occasional, thin coarser beds, referred to as the Pilong Formation

196 (Armitage & Viotti, 1977). More recent analysis has suggested that the Pliocene can be sub-divided into a lower, marine

197 interval, and an upper interval with greater non-marine influence, separated by a minor unconformity (Fig. 3) (Lunt,

198 2021), which is also consistent with seismic geomorphological evidence (Miall, 2022). There was a steady drop in

199 regional sea level throughout the Pliocene and Pleistocene, leading to permanent exposure of most of the Sunda Shelf

200 at around 400 ka, followed by several cycles of submersion and exposure (McGrath et al., 2023). During the lowstands,

201 a large river system developed flowed from the Gulf of Thailand, through the Malay Basin and towards the South China

202 Sea (Alqahtani et al., 2015, 2017; Miall, 2002; Twarog et al., 2021).

3. Data and Methodology

204 The data underpinning this work comes from decades of hydrocarbon exploration, appraisal, and production within

205 the basin. Almost all of the basin has been covered by 2D and 3D seismic surveys (Madon, 2021) and an extensive 3D

206 seismic dataset covering over 36,000 km^2 was available for this study (Fig. 4).

207 The dataset consists of ten seismic volumes of varying size and data quality. Record length varies from 4.5 s to 7.5 s,

208 the sampling interval varies between 2 and 4 ms and the inline/crossline spacing varies from 6.25 m to 25 m. Many of

209 these volumes are merged surveys, consisting of numerous smaller volumes already stitched together by a service

210 company. The largest of these is 23,000 km^2 in area and covers most of the central part of the basin. There was no

211 acquisition or processing information available other than those within file headers, and from visual inspection, it is

212 evident that there are varying degrees of signal quality and post-processing filtering from survey to survey.

213 Because of the large file sizes and computational power required to process such large seismic volumes, all volumes

214 were realized into 8-bit .zgy files within Petrel. This resulted in a significantly compressed file size, but no noticeable

215 change in data quality. A single velocity function was used to convert time-domain seismic interpretations to depth. To

216 obtain this function, a quadratic function was fitted to all available checkshot data within the Malay Basin (Fig. 5).
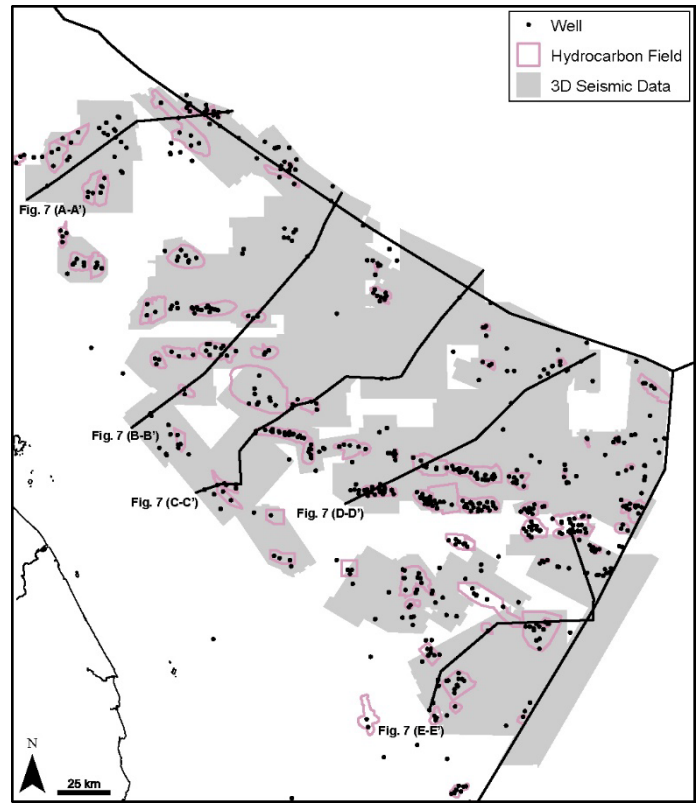
217

218
219

220

221
222

223 Previous studies addressing the structural evolution of the Malay Basin have been limited to observations from either

224 individual 3D seismic datasets or regional scale 2D seismic lines. Here, for the first time, we present analysis of a basin-

225 scale 3D seismic dataset. We started by mapping regional-scale seismic horizons across the entire dataset. These were

226 calibrated by stratigraphic tops picked from wells with time-depth data (checkshots) available and in some cases,

227 synthetic seismograms were created to improve or quality-control the seismic-to-well tie. For regional mapping, we

228 concentrated on mapping the tops of each Group (see subsequent section for an explanation of this nomenclature),

229 but detailed top structure maps were also constructed for other, locally prominent, intervals to describe key structural

230 features in certain areas of the basin. To aid the visualisation of geological structures, seismic variance maps were

231 extracted for the corresponding surface, and draped on top of the time-structure surface with layer blending to allow

232 visualisation of both.

233 The final step in our methodology was to review the trapping mechanisms for hydrocarbon discoveries within the

234 basin. This was undertaken to determine the different trapping domains within the basin and relate these to the

235 structural characteristics of the basin.

4. Results and Discussion

4.1. Basin Architecture

238 The seismic data available for our study allows us to focus mainly on the central-to-southeastern part of the Malay

239 Basin, offshore Malaysia (Fig. 4). The basin structure is best illustrated with a basin-wide top structure map for a

240 relatively deep horizon within Group K (Fig. 6) and long cross-sections along the main orientation of the structural dip

241 (Fig. 7).

242 The top basement horizon is a high amplitude, continuous to discontinuous seismic peak (downward increase in

243 acoustic impedance) representing a major unconformity separating folded Mesozoic rocks from the Cenozoic basin-fill

244 succession (Figs. 7, 8). The internal seismic character of the basement itself is varied, ranging from folded, laterally

245 continuous reflectors to chaotic, low-amplitude reflectors. This complex internal character is also supported by drilling,

246 where a range of rock types have been encountered (Madon et al., 2020). On the flanks of the basin, at depths of

247 around 2 s/2350 m or less, the top basement reflector is high amplitude, continuous and easily traceable (Figs. 7, 8).

248 At the southwest and northwest margins of the basin, there are deep faults that cut through the top basement horizon.

249 In the footwall to these faults, the basement dips into the basin centre and at depths of > 2 s, the horizon is either

250 difficult to interpret (discontinuous, low frequency and low amplitude) (Fig. 7) or deeper than seismic record length.

251 The basin has a very thick Cenozoic fill, particularly in the northwest where there are at least 4 s (~ 6.5 km) of Miocene-

252 Recent sediments preserved (Fig. 7, A, B and C). In the seismic profiles to the southeast, the Miocene interval is

253 significantly thinner (around 0.7 s/900 m), and this is accompanied by minor thinning of the Plio-Pleistocene

sequences, from around 1.2 s/1200 m thickness in the centre of the profile to around 0.8 s/700 m of thickness in the

southeast. Oligocene sequences are only mapped on the southwest, northeast, and southeast flanks of the basin.

Thickening and moderate structural uplift of the Oligocene sequences from southwest to northeast is observed from

around 600 ms/950 m thickness near the N-1 well to 2000 ms/3800 m thickness near the DY-1 well (Fig. 7E). Further

southeast, significant uplift of the Oligocene sequences brings these close to the Plio-Pleistocene interval near the LD-

1 well (Fig. 7E).

The basin has an asymmetric shape (Figs. 6 and 7). A series of basement-rooted, high-angle normal faults can be

observed along the southwest margin, which downthrow the basement by up to 500 ms/800 m and extend up into the

Pliocene sequences (Fig. 7B, C and E). In the hangingwall of these faults, the Oligocene-Miocene sequences dip steeply

into the basin with the deepest part of the basin located < 50 km away from this fault zone (Fig. 5, 6). By contrast, the

northeast margin has a much gentler dip (Fig. 7A, B and C).

The presence of discrete half-grabens within the basin can also be observed on these seismic profiles. The faults that

define these half-grabens affect mostly the Paleogene stratigraphy, with the greatest offsets at the top basement

horizon. Evidence for structural inversion can also be found, including reverse faults that affect the Paleogene interval,

folding of the Miocene interval and truncation beneath a prominent angular unconformity.
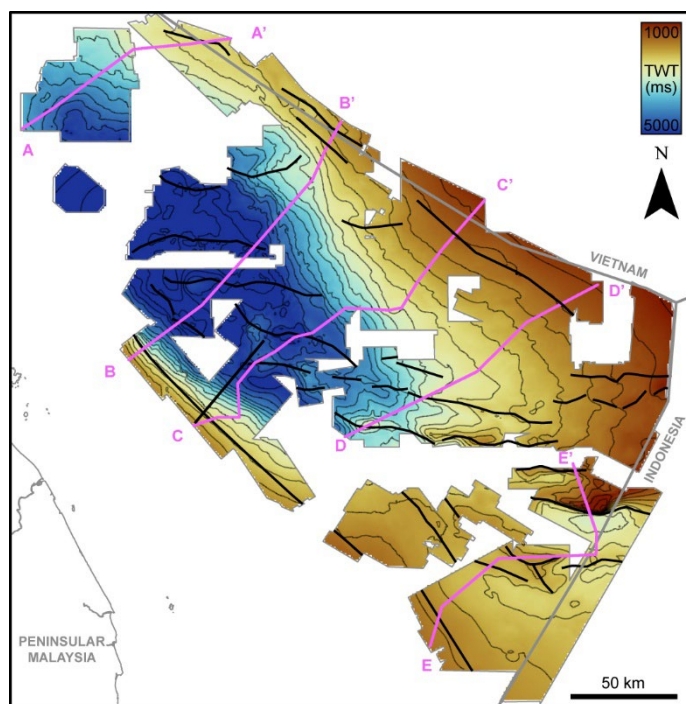
Figure 6: Intra-Group K time structure map with some major fault zones annotated (after Tjia (1994)). The locations of seismic cross-sections shown in Figure 7 are also shown.
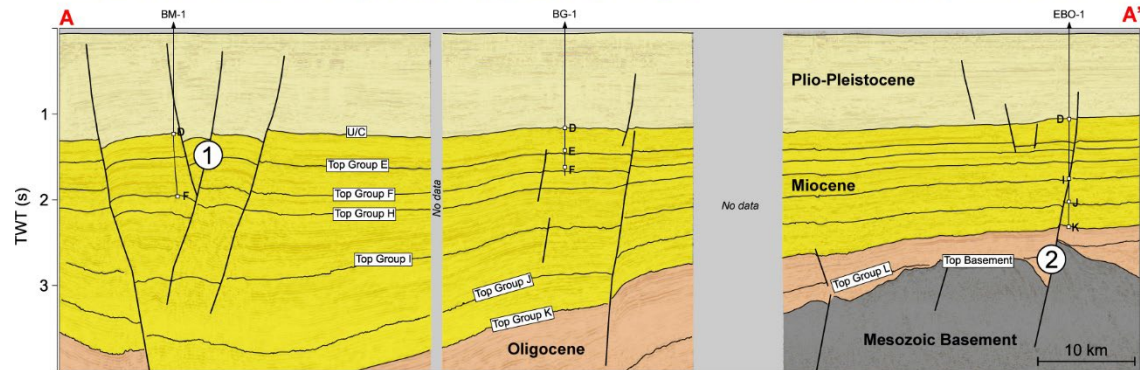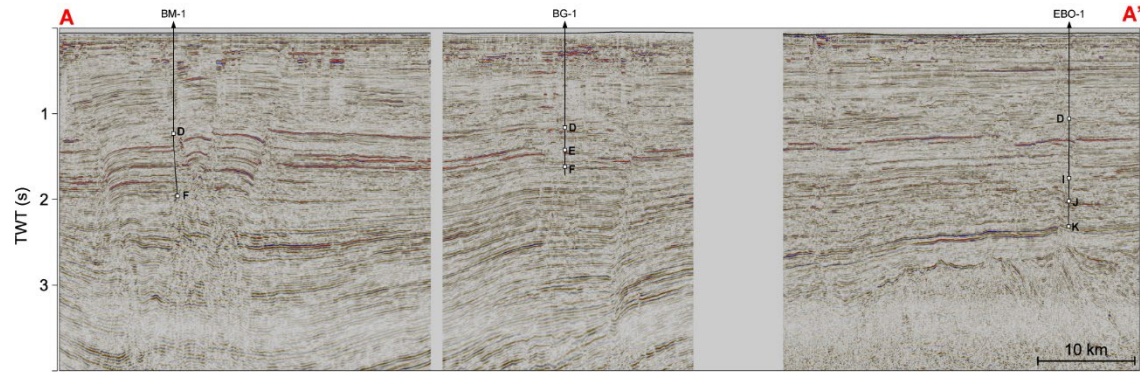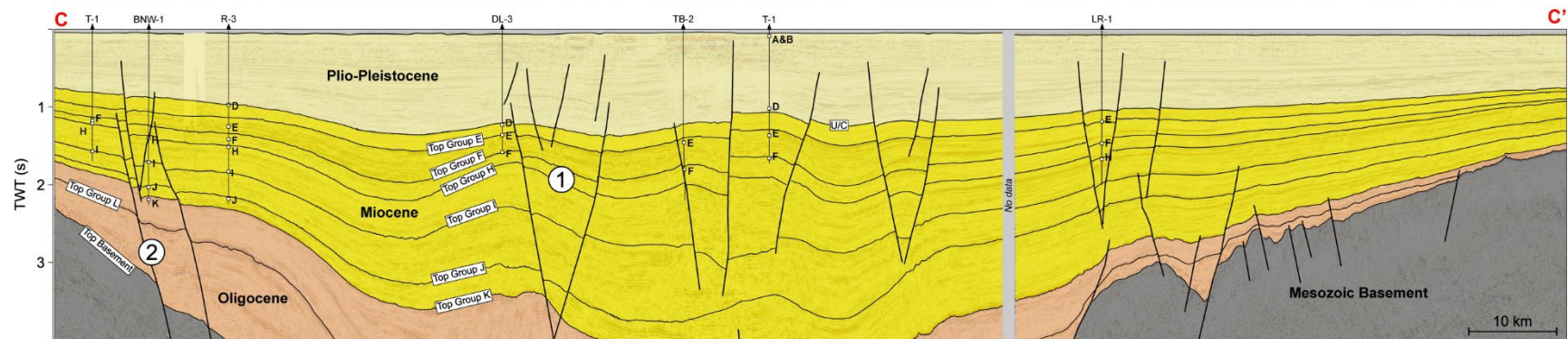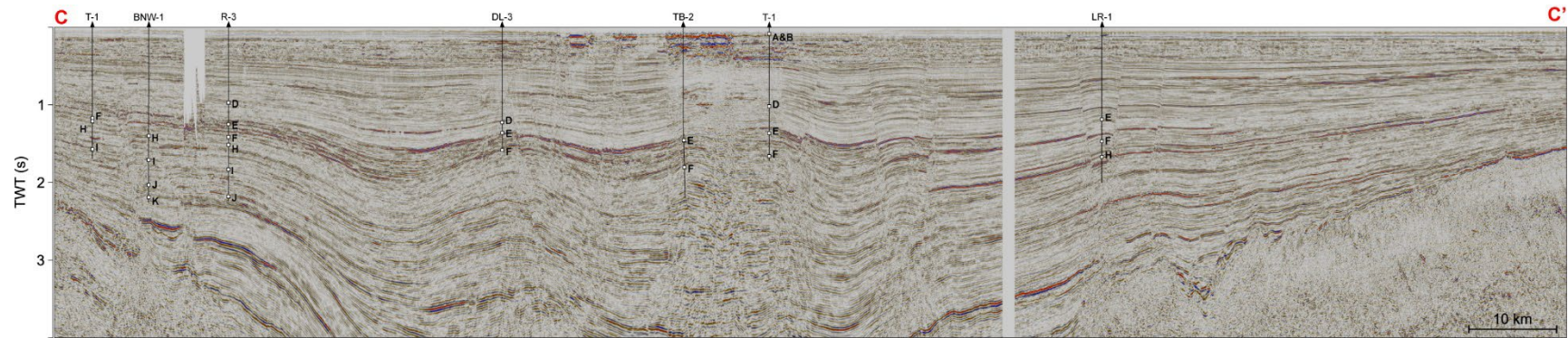
① Folded Miocene sequences cross-cut by younger extensionfal faults ② Basement-rooted, high angle normal faults that extend up to Pliocene
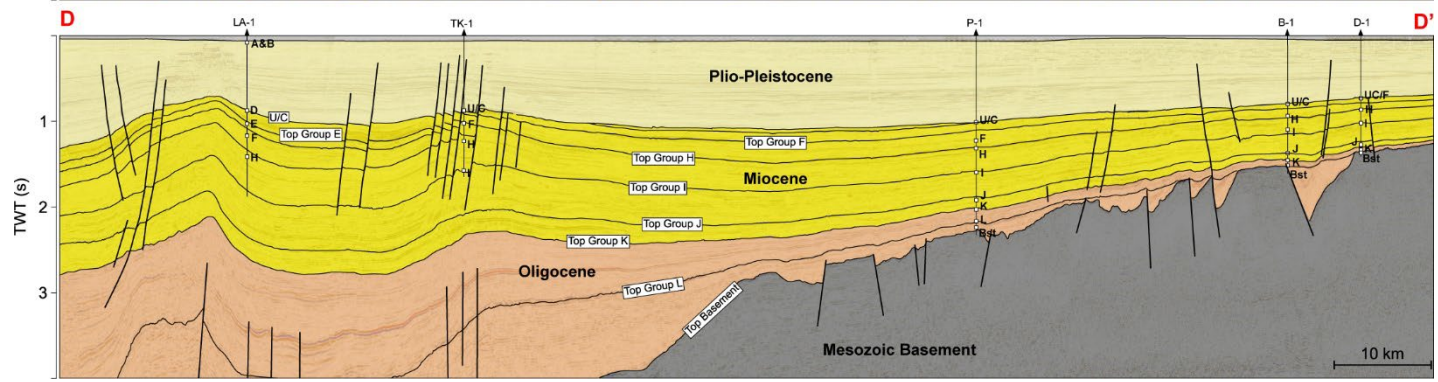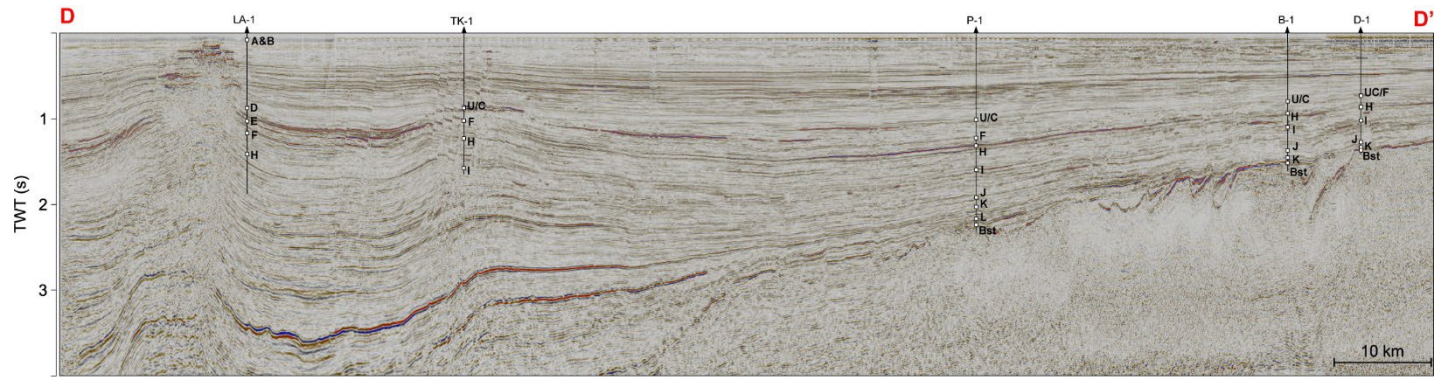
272
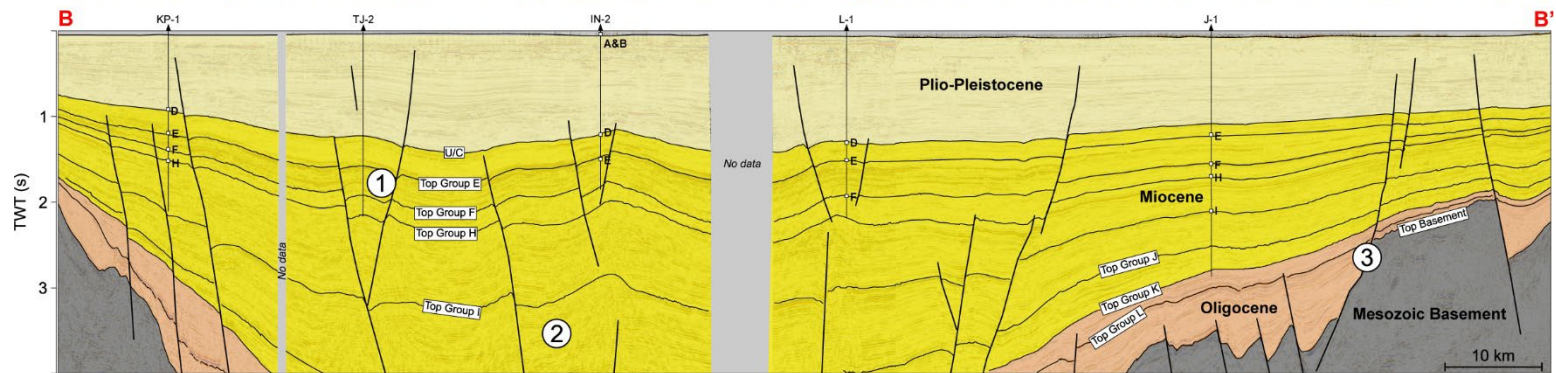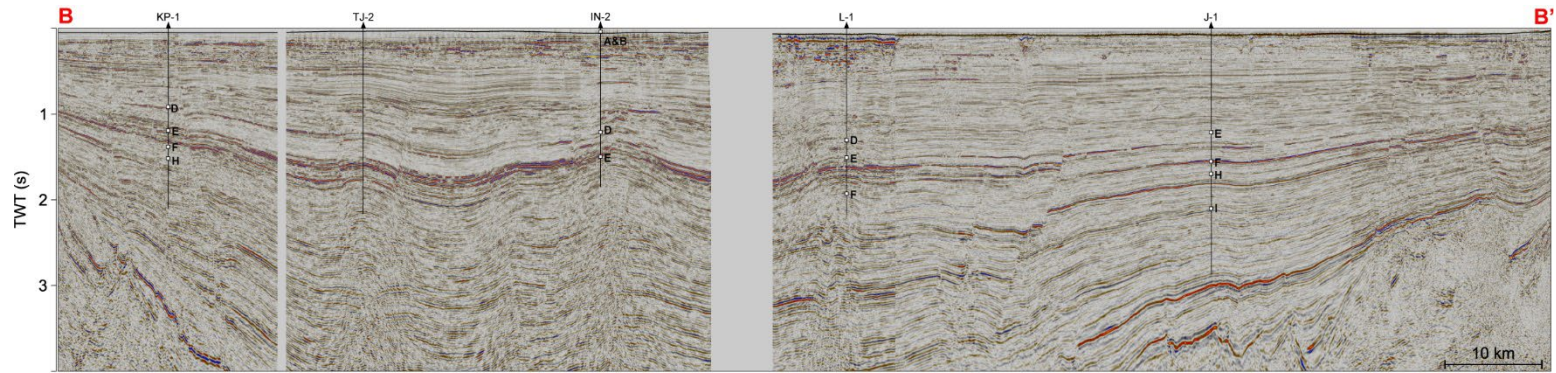
① Folded Miocene sequences cross-cut by younger extensional faults ② Thick Miocene-Recent sequence, > 4 s (c. 5 km) ③ Basement-rooted, high angle normal faults that extend up to Pliocene

① Folded Miocene sequences cross-cut by younger extensionfal faults   ② Basement-rooted, high angle normal faults that extend up to Pliocene

297
298
299
300
301
302
303
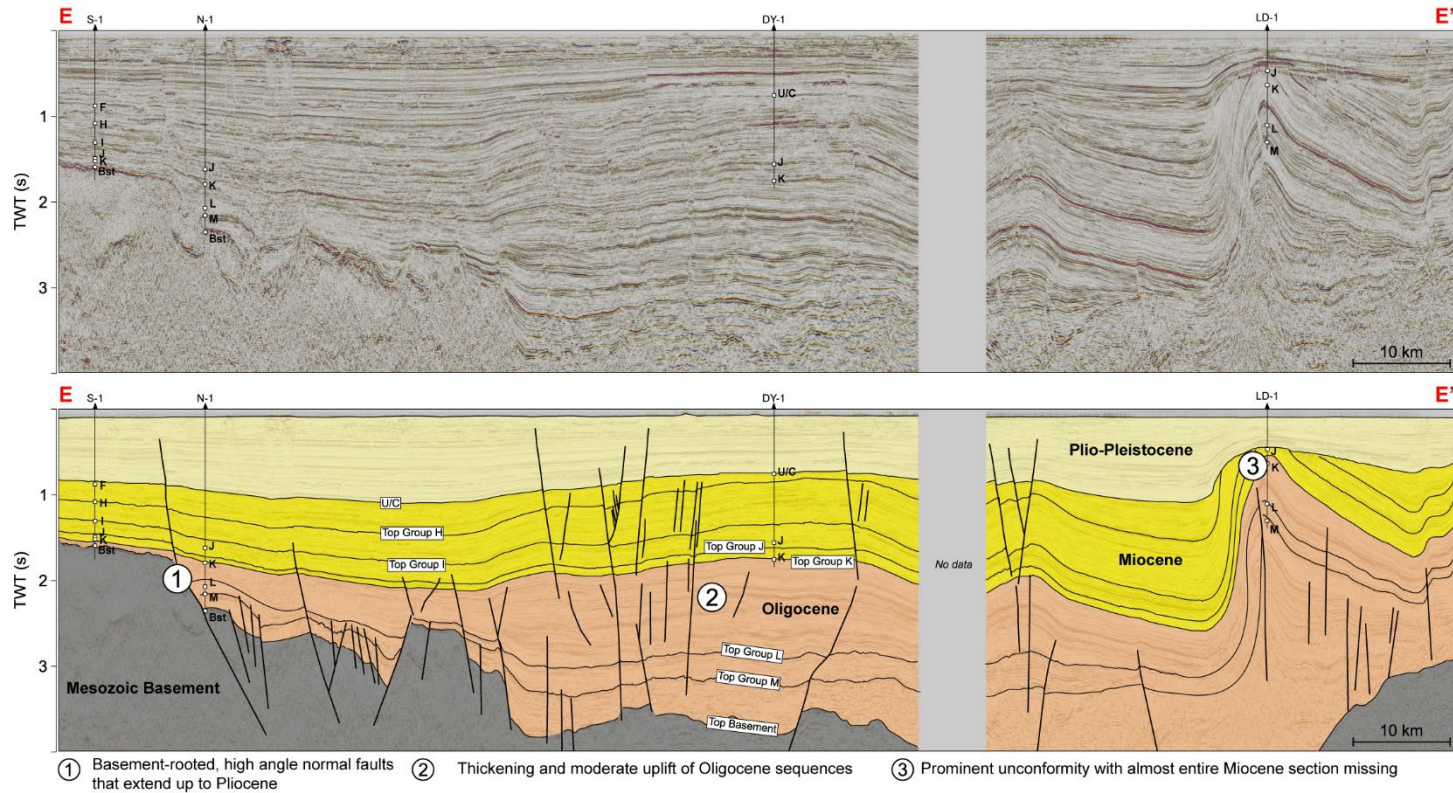304
305
306
307
308
309

310

311 *Figure 7: Un-interpreted (top) and interpreted (bottom) SW-NE-oriented regional seismic cross-sections (see Figs. 4 and 6 for the location of the lines). For simplicity, Group K to older is coloured as Oligocene in*
312 *age, but Group K extends into the earliest Miocene (Fig. 3).*

313

314

315

316

4.2. Paleogene Rifting and Transtension

The structural features of Paleogene half-grabens and grabens are demonstrated most clearly at the flanks of the basin (Fig. 7D, E). The faults that define these grabens tip out mostly within the uppermost Oligocene/lowermost Miocene interval and cut down through to the basement. The exception to this is at the hinge zones where these large offset basement-rooted faults extend up through the entire Miocene interval into the Pliocene interval. However, the throw in the Miocene and Pliocene is relatively minor, suggesting that the displacement is due to variable compaction rather than continued tectonic extension.

There are limited areas where the features of the initial, late Eocene W-E rifts can be studied. In most regions, the rifts have been deeply buried and/or structurally inverted. However, there is one area on the northeast flank of the basin where these features are clearly preserved (Figs. 7, 8). Here, a graben around 7 – 9 km wide and at least 50 km long is defined by two E-W-striking normal faults that downthrow the basement by > 1200 m.

The internal seismic characteristics of the graben-fill are a thick package of tilted, faulted, and folded reflectors that are mostly discontinuous and low amplitude with some notably bright intervals (e.g., at the base). The fill is also highly structured. Some normal faulting can be observed, but there is also evidence of compression in the way of reverse faults, folding and reflector truncations (discussed in subsequent sections) (Fig. 8). This graben lacks stratigraphic well control, however, it likely contains Eocene age (Groups L and older) continental clastic deposits observed in other parts of the basin.

There is also clear evidence from the seismic data of dextral fault movements, notably along the WHFZ (Fig. 9). In most instances, a NW-SE-striking deformation zone can be identified, but faults of varying geometry and size are also present (Fig. 9). At the northwestern part of our dataset (Fig. 9A, B), strike-slip characteristics are visible even at very shallow depths (Fig. 9A). Here, long faults curve around from NW-SE to N-S (~ 20 ° clockwise) with throws of up to 50 m. At deeper levels, long normal faults can also be observed (Fig. 9B), but some antithetic and slightly oblique normal faulting creates small grabens with minor structural inversion.

In the SE of the basin, a cluster of small E-W fractures are oriented around 75 ° to two NW-SE-striking faults (Fig. 9C). The orientation of these fractures suggests a link to the earlier Paleogene rifting phase within the basin. Further south, very distinct en echelon fault geometries can be observed, consisting of multiple NNW-SSE Riedel shears and short SW-NE extensional faults (Fig. 9D).
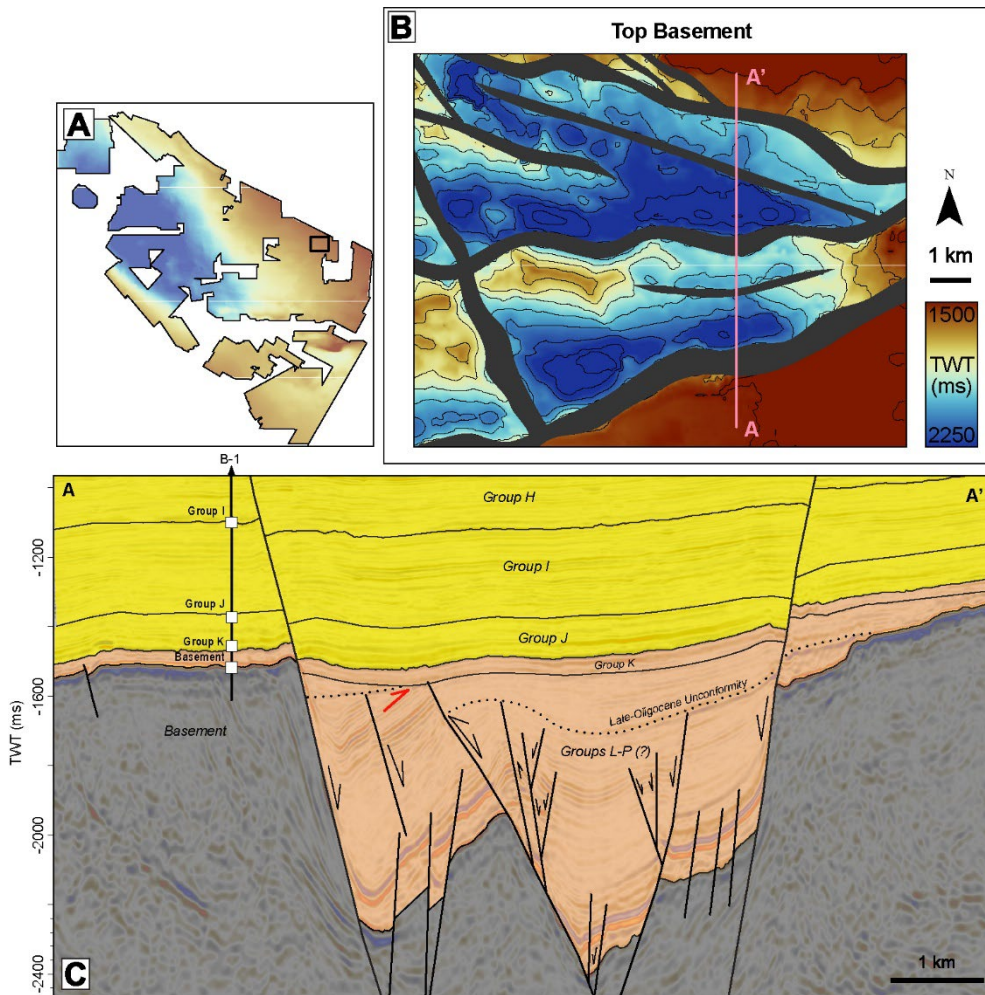
344
345   *Figure 8: A series of illustrations highlighting the structure of a Paleogene graben north of the B-1 well. (A) Regional location map showing the*
346   *location of B, (B) Top structure map, in two-way-time (TWT), for the basement horizon, (C) S-N-oriented seismic cross-section highlighting the*
347   *seismic characteristics of the graben-fill.*
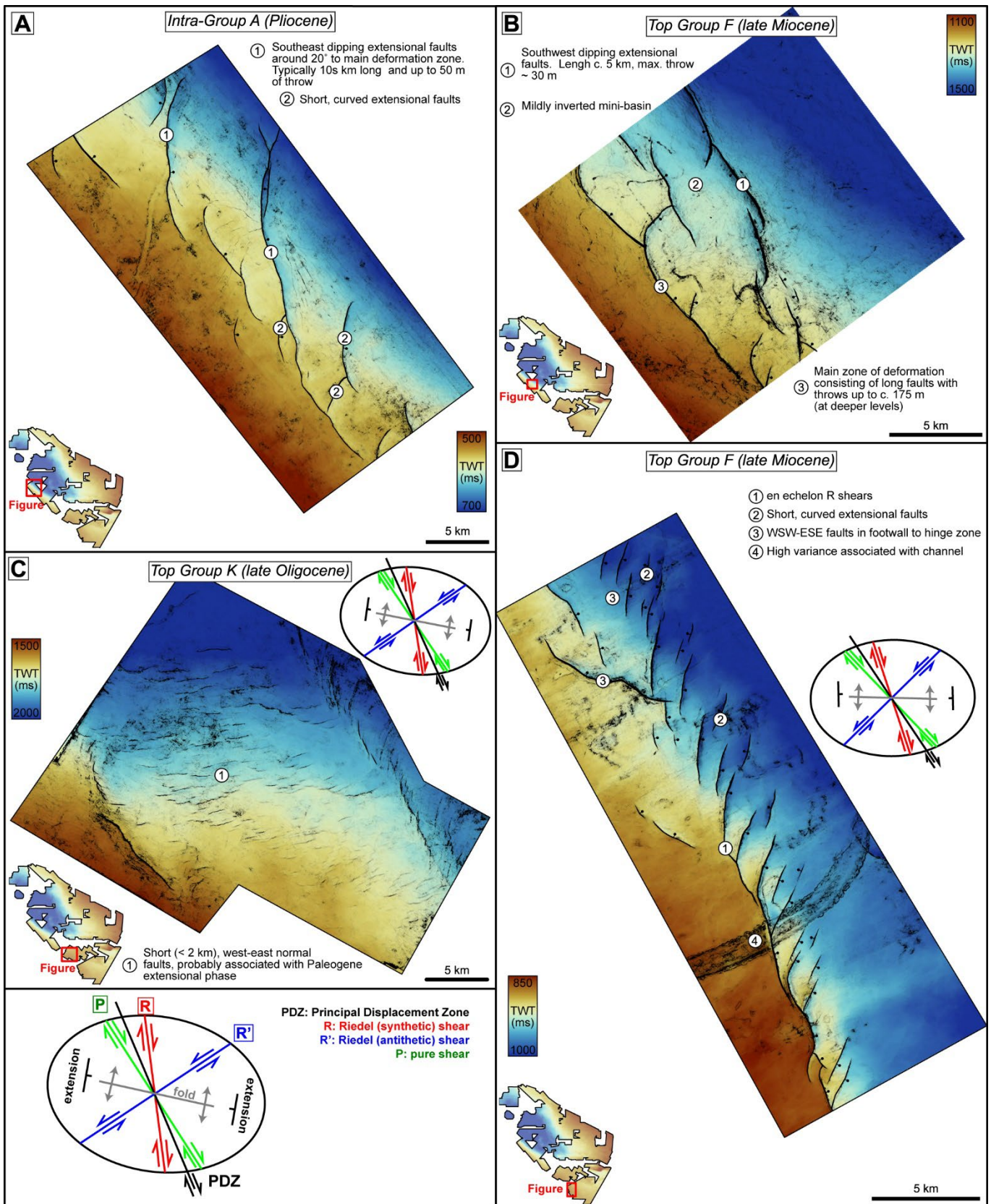
Figure 9: Top structure maps for four areas that illustrate strike-slip characteristics along the Western Hinge Fault Zone. The red-to-blue colour bar represents the depth of the surface in two-way-time (TWT). The maps also contain a layer-blended seismic variance map for the corresponding horizon. Here, black colours indicate high seismic variance (low continuity - faults) and low seismic variance is transparent.

4.3. Neogene Inversion

The structural expression of two separate uplift events can be observed within the basin. The first event is tentatively dated as late Oligocene and evidence is found on the flanks of the basin. In Figure 8, evidence for uplift (reverse faulting,

folding) and erosion (truncation) can be observed towards the top of the syn-rift sequence, but the graben lacks biostratigraphic age constraints from wells to accurately date this event. The unconformity is probably equivalent to the late Oligocene unconformities observed in the West Natuna (Ginger et al., 1993) and Penyu (Madon et al., 2019) Basins. Several authors have attributed this uplift event to the breakup of the South China Sea (Ginger et al., 1993; Morley, 2016; Morley et al., 2003).

The most prominent evidence for structural uplift is the folding of Miocene sequences and a locally deep unconformity, the Intra-Late Miocene Unconformity (ILMU). These folds form within a belt that runs through the centre of the basin (Fig. 2), with their long axis striking W-E. They are associated with deeper W-E-striking faults (Fig. 2), an example of which can be observed in the southwest part of Figure 7D beneath LA-1 well. In this instance, a deeper reverse fault can be seen with the Miocene fold axis positioned above its hangingwall. This suggests that these folds were from fault propagation, even though these faults are often too deeply buried in other parts of the basin to confirm this. There is little-to-no inversion of the western basement-rooted fault (Fig. 7B, C, E) or faults along the eastern flank, with folding restricted to the central and deeper areas of the basin.

The folds are often crosscut by younger extensional faults that sole out mostly within the Miocene interval itself (Fig. 7). The most dramatic evidence for compression and uplift is in the vicinity of LD-1, where almost the entire Miocene interval has been removed and there is a prominent angular unconformity with the Plio-Pleistocene interval above (Fig. 7E). Towards the NE edge of this regional line, strong inversion and uplift around L-1 well can be observed, with the ILMU cutting down to intra-Group J. Looking in more detail at the area around the P-1 well (Fig. 10), WNW-ESE-striking faults have experienced strong inversion with > 60 m of reverse displacement at Group K level (Fig. 10C). This produces large, WSW-ESE-striking anticlines with very steep limbs on the south-side (Fig. 10B). Small offset faults also affect the hangingwall, striking SW-NE, NW-SE, and WSW-ENE. These faults appear to have retained normal displacement sense.
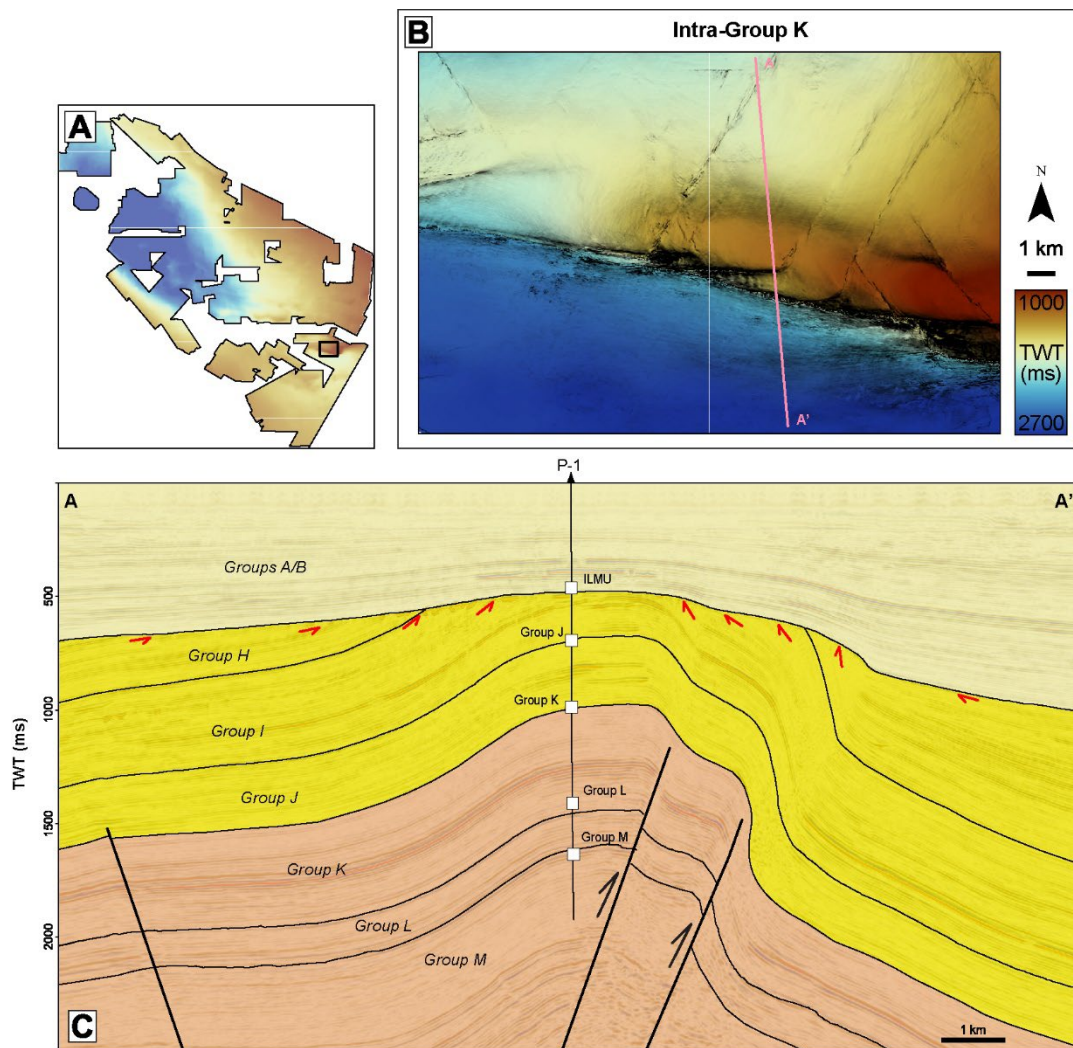
382 The ILMU cuts through various intervals from the Miocene down to the late Oligocene (Fig. 3). To study this further,

383 the subcrop to this unconformity was mapped using well penetrations and seismic mapping (Fig. 11). Over much of

384 the basin, the unconformity has only removed part of the Tortonian; Group D is preserved as a subcrop. In the east

385 part of the basin, the unconformity is underlain by middle Miocene units (Groups F and H). This equates to a time gap

386 of ~5-8 My or a missing section of ~ 1500 – 2400 m assuming 300 m/Ma as a reasonable average post-rift sedimentation

387 rate in the basin (Madon, 2007, Figure 12(b)).

388 The deepest erosion is limited to a small region in the SE, where the unconformity cuts down to Group K. This is a time

389 gap of ~14 My, which could represent a missing section of up to 4200 m of (following the same assumptions as stated

390 above). This is significantly higher than previous estimates of the extent of uplift in this region, (e.g. 1200 m; Du Bois,

391 1985).
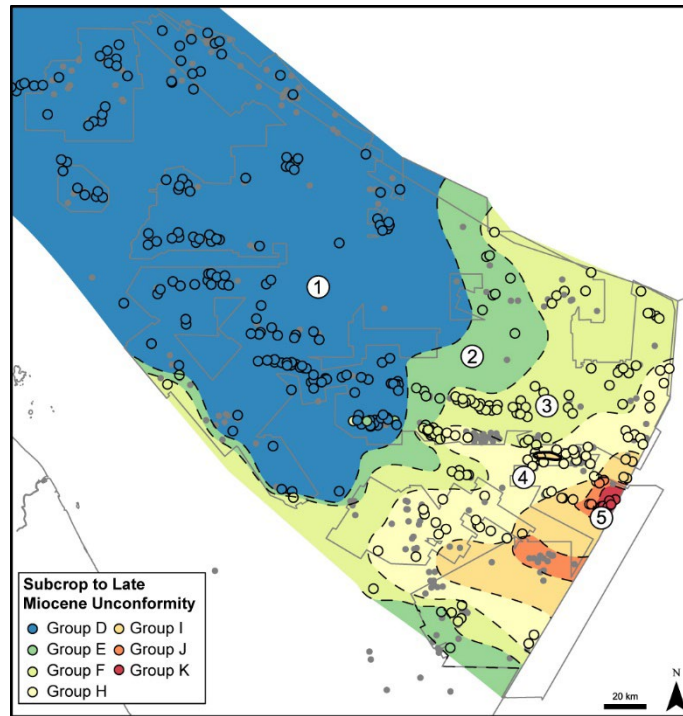
Figure 11. 1: 0.5 My time gap, ~150 m missing section, 2: 1.5-5 My time gap, ~450-1500 m missing section, 3: 5-7.5 My time gap, ~1500 – 2250 m missing section, 4: 7.5-9.5 My time gap, ~2250-2850 m missing section, 5: up to 17 My time gap, up to ~5 km missing section

In the central part of the basin, the ILMU is less clear and separates Messinian Group A&B sediments from Tortonian sediments belonging to Group D (Fig. 3). In these areas, inversion of deeper grabens has generated anticlines, but without the deep erosive event observed in the southeast of the basin. In some areas (Fig. 12B), Oligocene horizons can still be mapped with confidence. In addition, W-E-striking reverse faults can be observed, with anticlines developed within their hanging walls. These anticlines form along a set of ridges; a reflection of the original (now inverted) narrow rift system (Fig. 2). In deeper areas of the basin, the syn-rift sequences are too deeply buried to be mapped, but anticlines can be mapped within the middle-upper Miocene stratigraphy (Fig. 12A). Here, many of these anticlines are also crosscut by short, curved extensional faults.
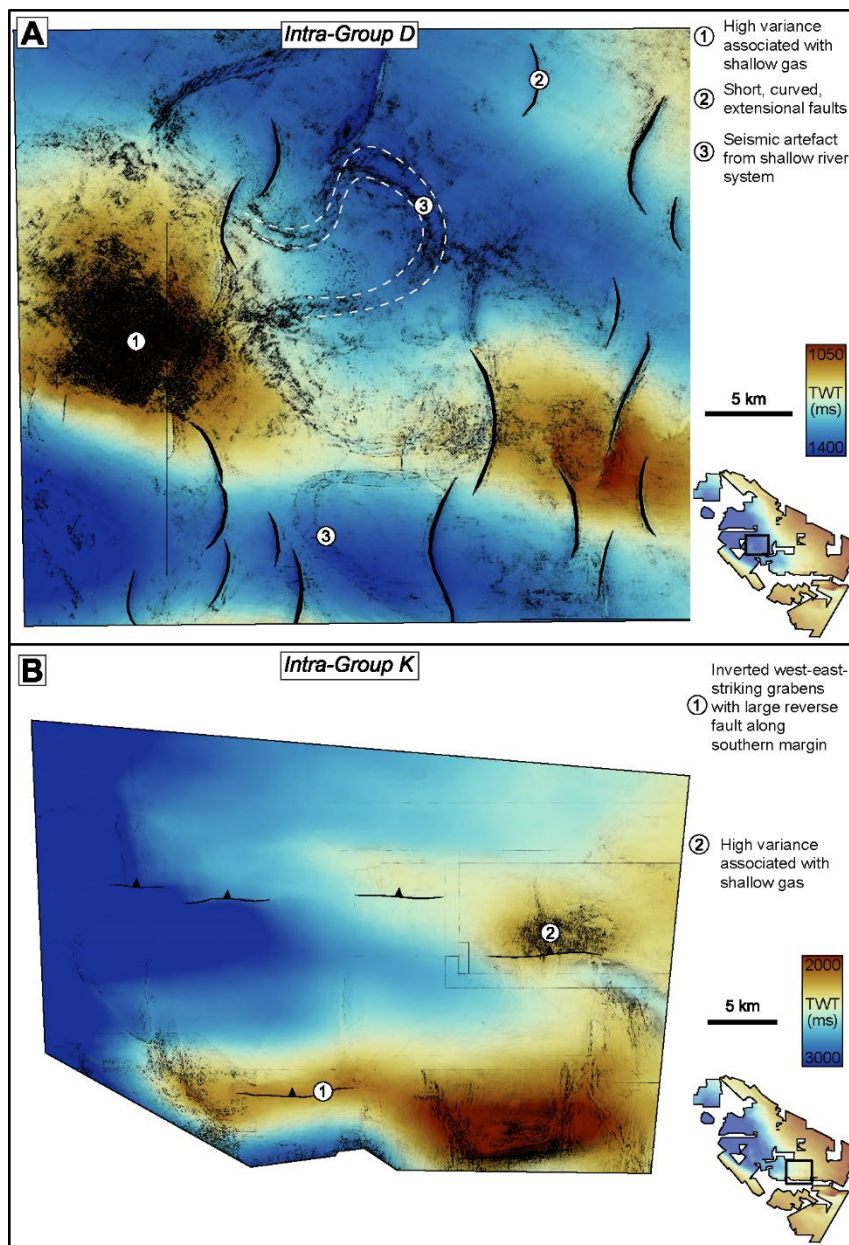
404 *Figure 12: Top structure maps for two areas over anticlines in the centre of the basin. The red-to-blue colour bar represents the depth of the*
405 *surface in two-way-time (TWT). The maps also contain a layer-blended seismic variance map for the corresponding horizon to highlight faults or*
406 *other seismic discontinuities such as gas clouds.*

4.4. Plio-Pleistocene Characteristics

Evidence for tectonic quiescence during the Pliocene can be observed on a regional scale. Seismic horizons above the ILMU dip gently across the basin, generally < 1 °, though there is some deformation above the E-W belt of anticlines (Fig. 13). This is in marked contrast to reflectors beneath the ILMU, which show much more deformation, with the steepest dips (> 10 °) being associated with the Western Hinge Zone and the E-W anticlines (Fig. 14B).

However, there are some subtle indications of structural events affecting the basin during this period. Some authors have noted a minor intra-Pliocene unconformity (IPU) within wells located in the southeastern Malay and West Natuna Basins (Armitage & Viotti, 1977; Lunt, 2021). One such well was Pulai-1, in which Armitage and Voitti (1977) inferred the IPU based on the absence of palynological zone N20 within the Pilong Fm (Group A&B) (Fig. 3), and a high amplitude

416   seismic event around the well (Fig. 14). This seismic event is at 475 ms TWT (385 m MD in the well), some 100 ms

417   shallower than the ILMU (around 555 ms TWT or 460 m MD in the well, Fig. 14). Lunt (2021) discussed that the IPU

418   could result from a regional drop in base level associated with stronger glacio-eustatic control during the mid-Pliocene.

419   An upward decrease in the Gamma Ray (GR) log within the interval beneath the IPU at Pulai-1 (Fig. 14) could be

420   interpreted as a regressive event, aligning with other authors' observations of a shallowing in depositional facies up

421   through the Pliocene (e.g., West Natuna Basin: Darmadi et al., 2007 and Nam Con Son Basin: Matthews et al., 1997).
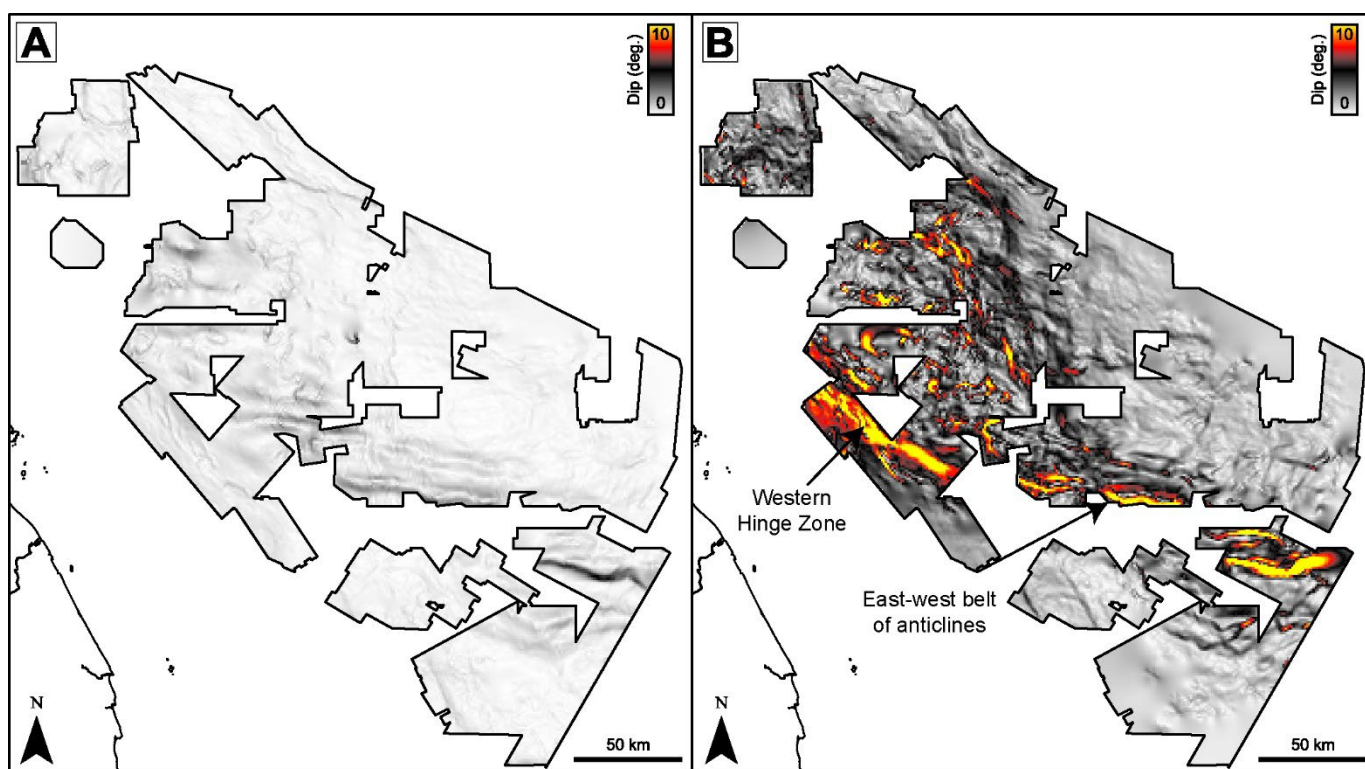
422

423   *Figure 13: Dip maps for an intra-Pliocene horizon (A) and intra-Oligocene horizon (B) with identical colour scaling.*
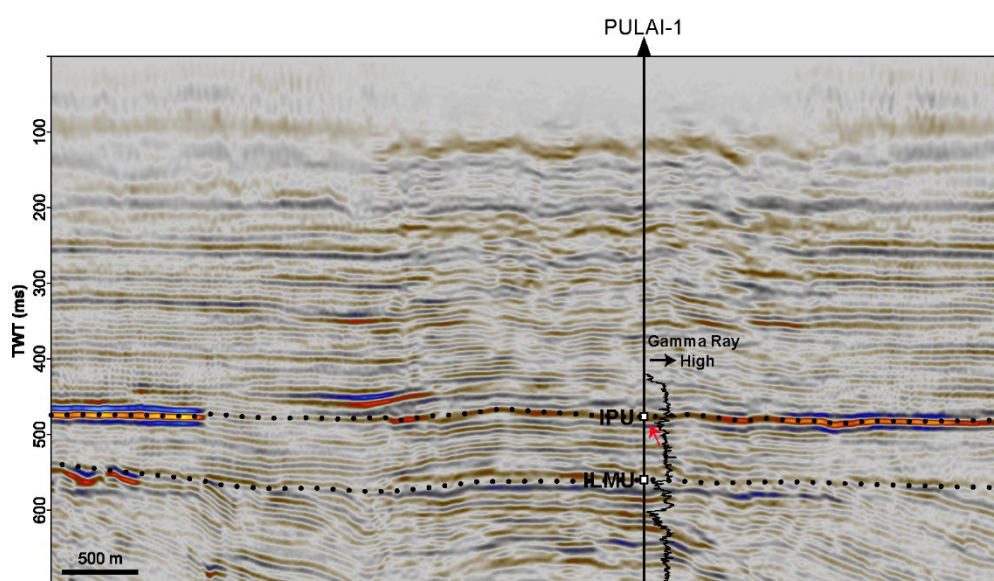
424

425   *Figure 14: Southwest-northeast oriented cross-section through Pulai-1 well*

426   There is also evidence of structural deformation in the deeper part of the basin to the north. Previous authors have

427   noted a N-S-striking fault zone that particularly affects the central and western parts of the basin (Liew, 1997; Tjia,

428   1994). This zone has been used to broadly separate the Malay Basin into a northern domain consisting of N-S-striking

429   faults and a southern domain consisting of E-W-striking faults (Fig. 2) (Liew, 1997; Tjia & Liew, 1996). The structural

430   characteristics of this area can be observed from a top structure map of the ILMU near Ular field (Fig. 15), which lies

431   within the N-S-striking Kapal-Bergading and Kuda-Ular fault zones (Tjia & Liew, 1996). Here, many long (10 - 20 km)

432   curvilinear faults with throws up to ~200 m crosscut the ILMU with orientations around N-S to NNE-SSW (Fig. 15). It is

433   difficult to ascertain if these faults extend down to the basement, due to its burial depth, but the faults appear to cut

434   through most of the Oligocene-Miocene fill and previous authors have suggested these fault zones formed following

435   reactivation of N-S basement faults akin to those onshore Peninsular Malaysia (Liew, 1994; 1997). Some shorter (mainly

436   < 5 km) faults also affect anticlines within the centre of the basin (e.g., Fig. 12). These have previously been attributed

437   to crestal collapse, following the Upper Miocene compressional events (Tjia, 1994).

438
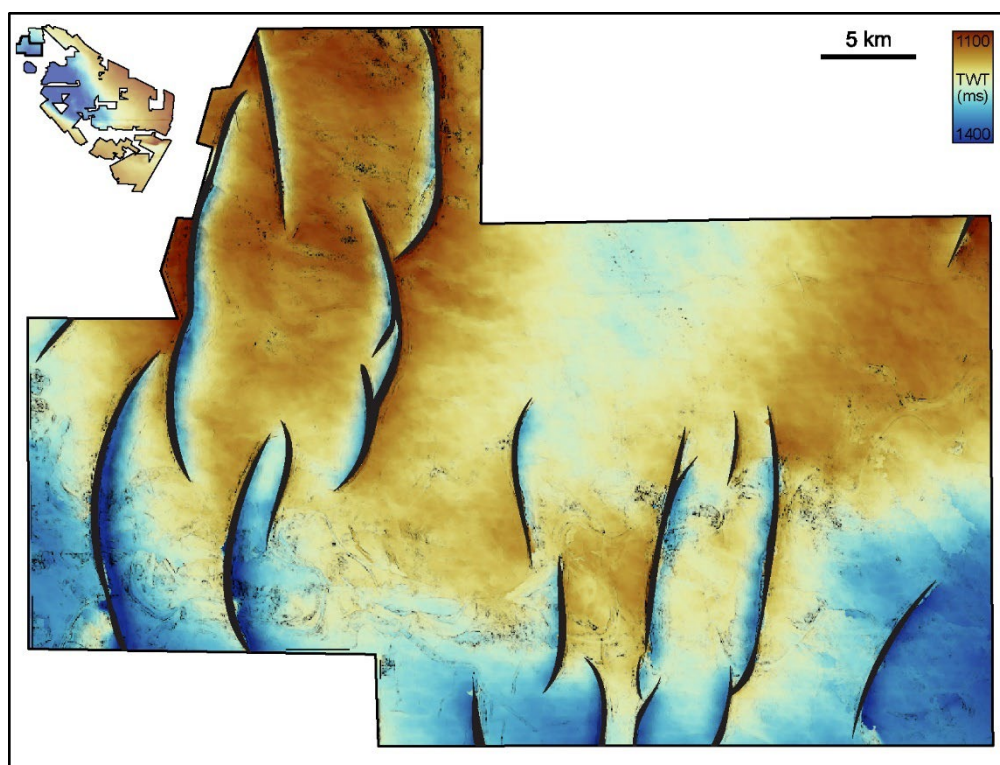
439 *Figure 15: Top structure map for an area in the northwest of the basin. The red-to-blue colourbar represents the depth of the surface in two-*
440 *way-time (TWT). The maps also contain a layer-blended seismic variance map for the corresponding horizon to highlight faults and other*
441 *seismic discontinuities.*

442   During this period of steady subsidence, accommodation space within the Malay Basin was quickly filled. It is suggested

443   that by the late Pliocene fluvial systems bypassed the basin entirely and instead flowed east towards the Nam Con Son

444   Basin and the South China Sea (Murray & Dorobek, 2004). However, as noted above, a significant sea level drop

445   occurred within the Pliocene leading to the resumption of fluvial deposition in the Malay Basin. Global cooling during

446   the Pleistocene led to a gradual drop in sea level, exposing the Sunda Shelf. However, by late Pleistocene (250 ka), the

447 shelf was repeatedly submerged and exposed (McGrath et al, 2023) because of high-amplitude glacio-eustatic sea-

448 level fluctuations.

4.5. Trap Analysis and Implications for CCS

450 Following the development of a structural and stratigraphic framework for the basin, we re-evaluated the main

451 trapping mechanisms within existing hydrocarbon fields. The rationale for this is to constrain which trap types might

452 be better suited to CO_2 storage (i.e. those with high capacity and low containment risk) and how these are distributed

453 across the basin.

454 To achieve this, the main trapping mechanism for ~ 200 hydrocarbon discoveries was analysed systematically by

455 integrating the results of our mapping with descriptions from well reports and previous studies where available. A

456 scheme modified slightly from Vincelette et al (1999) was adopted, which led us to classify 12 different trap types (Fig.

457 16). Around one third of traps were within folds developed in association with inversion of deeper fault zones (Fig.

458 16B). These traps consist of several stacked reservoir horizons folded into a four-way dip closure (Fig. 16E), forming

459 some of the largest oil and gas discoveries in the basin (Madon, 2021). They form a belt that runs E-W from the

460 maritime border with Indonesia towards the centre of the basin where it bends upwards to run parallel with the

461 shoreline of Peninsular Malaysia (Fig. 16A). Most of these folds are oriented E-W (28 %), but some are also oriented

462 NW-SE and SW-NE, located mainly to the south and southeast areas of the basin, respectively.

463 While the largest structural traps in a basin may be obvious targets for CO_2 storage, the presence of shallow gas above

464 many of these anticlines must be seen as a significant risk for storage containment that requires further analysis.

465 Intervals of high seismic variance, high noise, and low reflector continuity overly these anticlines (Fig. 12A) which

466 strongly implies breach of these structural traps. At the moment it is not clear what the rate of leakage is (and if this is

467 of concern for storage, or not) or if the leakage mechanisms are via small faults or by advection through the caprock

468 matrix when overcoming the capillary entry pressure.

469 Fault-associated traps are the other dominant trapping mechanism in the basin, accounting for ~ 45 % of our analysed

470 discoveries (Fig. 16B). Here, we include anticlines developed within the hangingwall of extensional faults (rollover

471 anticlines), and tilted fault blocks that rely on some element of fault seal either across the hangingwall or the footwall

472 (Fig. 16D). In the case of the former, these are more prevalent in the north and northwest of the basin where they are

473 often associated with N-S-striking faults such as the Kuda-Ular fault zone (see section 4.4). In some cases, a single fault

474 will have a rollover anticlinal trap and a footwall tilted fault block trap associated with it, as shown by the pairing of

475 each trap type in the northwest of the basin (Fig. 16A, D). Tilted fault block traps in the Malay Basin are usually fairly

476 small and this combined with the requirement for a lateral fault seal, probably makes them less attractive targets for

477 CO_2 storage. Determining fault seal efficacy would require analysis of geometry, juxtaposition and host rock properties

478 either side of the fault, and the presence of hydrocarbon accumulations within shallow intervals associated with these

479 faults is evidence that fluid flow up some faults in the basin is possible. While rollover anticlines are by definition

480 associated with a fault, the closures are often purely formed by structural dip and are thus lower risk traps.

481 Traps that relate to a basement high are preferentially located at the edges of the basin (Fig. 16A). These include those

482 formed by structural drape of sediments over a basement high. These traps are mostly low-relief and mainly

483 constrained to the Oligocene- lower Miocene horizons (Fig. 16C). These traps do not show the same evidence for fluid

484 leakage as the large anticlinal traps, but on the other hand, are much smaller in size. Fractured basement and traps

485 with an up-dip seal against a basement high are only documented in a few cases and are unlikely to be serious targets

486 for CO_2 storage in lieu of lower risk locations. The latter two are only documented in a few cases and structural drape

487 is the dominant mechanism (12 % of our total analysed discoveries).

488 Structural trapping is an important mechanism for CO_2 storage within aquifer systems. Upon injection into an aquifer,

489 the CO_2 plume will migrate up-dip, filling any structural traps successively in a concept often referred to as a "trapping

490 chain". Each structure will have its own associated risk of leakage. For example, large fold traps in the Malay Basin are

491 often associated with seismic features indicative of shallow gas and leakage from the reservoir. Fault-seals can also

492 bring inherent risks that need to be analysed on a case-by-case basis, accounting for fault geometry and rock properties

493 to assess their leakage potentials. By identifying the domains shown in Figure 16, we provide an initial indication of the

494 trapping styles expected within certain parts of the basin, and a concept that can be tested with subsequent plume
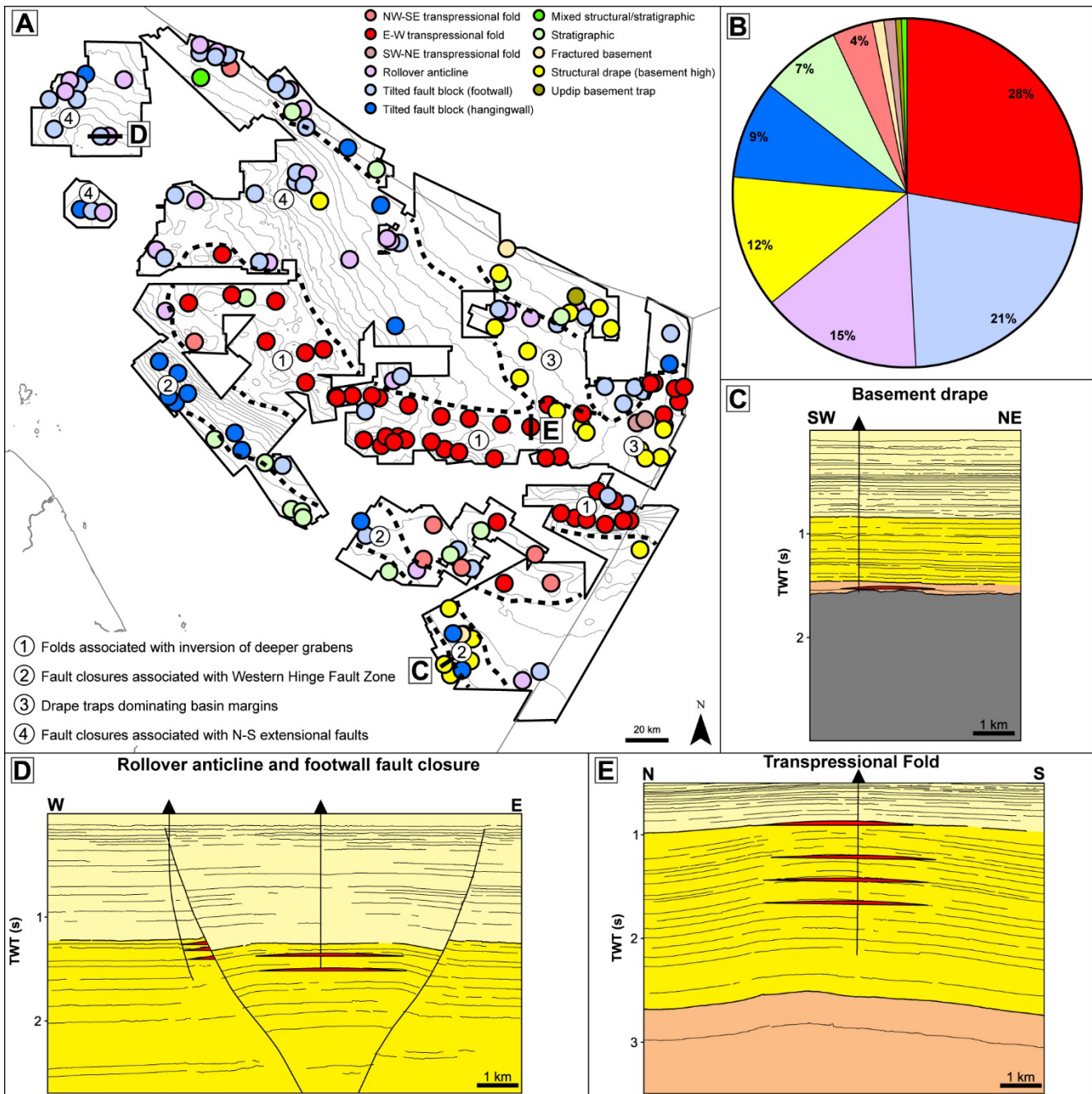
495 migration simulations.

Figure 16: Classification of ~ 200 discoveries by trap type shown in map view (A) and as a pie chart (B). Examples of the main trap types are also shown in the form of structural cross-sections from seismic data (C, D, E). Base contours in (A) are taken from Figure 6 (intra- Group K horizon)

5. Conclusions

Using newly available, regional, 3D seismic and well data for the Malay Basin, we present a detailed analysis on the structural and stratigraphic evolution of the basin and consider implications for CO_2 storage potential.

Rifting started occurred during the late Eocene when sinistral motion across NW-SE-striking strike-slip faults produced W-E-striking faults and narrow sub-basins. These basins were filled with Eocene-Oligocene continental clastic sediments before a late Oligocene compressional event uplifted and folded these sequences to produce an angular unconformity. More widespread opening of the basin started during the late Oligocene when dextral motion across NW-SE-striking strike-slip zones generated N-S-striking en-echelon faults and ridges. Strike-slip deformation is evident

along the Western Hinge Zone and consists of en-echelon faults, oblique shear faults and perpendicular tensional fractures. Following a tectonically quiescent post-rift phase, two prominent unconformities are present during the middle-late Miocene. A middle Miocene unconformity has removed parts of Group E and is likely linked to sea level fall associated with the emergence of the Natuna area to the southeast. Inversion occurred throughout the late Miocene, culminating in a regional unconformity with up to 5 kilometres of Miocene sediments eroded in the SE of the basin. There was little tectonic activity during the Pliocene-Pleistocene, but some faulting affects the northwest of the basin and there is some evidence of an intra-Pliocene unconformity generated by regional sea level fall.

These new structural and stratigraphic observations allow us to delineate several trapping domains across the basin. These trapping domains help us to identify areas where additional structural closures may exist within saline aquifers that could be targets for CO_2 storage. Future work should involve more detailed analysis of trapping styles and seal efficacy to de-risk potential containment issues associated with shallow gas.

References

Abd Rahman, I. Z., Abang Hasbollah, D. Z., Mohd Yunus, N. Z., Kasiman, E. H., & Mazlan, A. N. (2022). Carbon dioxide storage potential in malaysian sandstone aquifer: An overview. *IOP Conference Series: Earth and Environmental Science*, 971(1), 012022. https://doi.org/10.1088/1755-1315/971/1/012022

Ahmed Satti, I., Wan Yusoff, W. I., & Ghosh, D. (2016). Overpressure in the Malay Basin and prediction methods. Geofluids, 16(2), 301–313. https://doi.org/10.1111/gfl.12149

Almasgari, A. A., Elsaadany, M., Latiff, A. H. A., Hermana, M., Rahman, A. H. B. A., Babikir, I., Imran, Q. S., Appiah, N. F., & Adeleke, T. O. (2020). Application of seismic attributes to delineate the geological features of the Malay Basin. *Bulletin of the Geological Society of Malaysia*, 69, 97–110. https://doi.org/10.7186/bgsm69202009

Alqahtani, F. A., Johnson, H. D., Jackson, C. A. -L., & Som, M. R. B. (2015). Nature, origin and evolution of a late pleistocene incised valley-fill, sunda shelf, southeast asia. *Sedimentology*, 62(4), 1198–1232. https://doi.org/10.1111/sed.12185

Alqahtani, F. A., Jackson, C. A.-L., Johnson, H. D., & Som, M. R. B. (2017). Controls on the geometry and evolution of humid-tropical fluvial systems: Insights from 3d seismic geomorphological analysis of the malay basin, sunda shelf, southeast asia. *Journal of Sedimentary Research*, 87(1), 17–40. https://doi.org/10.2110/jsr.2016.88

Argus, D. F., Gordon, R. G., & DeMets, C. (2011). Geologically current motion of 56 plates relative to the no-net-rotation reference frame: NNR-MORVEL56. *Geochemistry, Geophysics, Geosystems*, 12(11), n/a-n/a. https://doi.org/10.1029/2011GC003751

Armitage, J. H., & Viotti, C. (1977). Stratigraphic nomenclature-southern end Malay basin. *Proc. Indon Petrol. Assoc., 6th Ann. Conv.* Sixth Annual Convention. https://doi.org/10.29118/IPA.1281.69.94

Arshad, A.R.M., Mhd, D., & Tjia, H.D. (1995). A deep seismic section across the Malay Basin: Processing of data and tectonic interpretation. *Warta Geologi (Newsletter of the Geological Society of Malaysia)*, 21(6), 412.

Babikir, I., Salim, A. M. A., Hermana, M., Abdul Latiff, A. H., & Al-Masgari, A. A.-S. (2022). Characterizing the subsea Pleistocene fluvial system of the Sunda shelf, offshore Malaysia, using multiattribute corendering and self-organizing maps. *Interpretation*, 10(2), T291–T304. https://doi.org/10.1190/INT-2021-0005.1

543 Bird, P. (2003). An updated digital model of plate boundaries. *Geochemistry, Geophysics, Geosystems*, 4(3),
544   2001GC000252. https://doi.org/10.1029/2001GC000252

545 Bishop, M. (2002). Petroleum systems of the Malay Basin Province, Malaysia. *Open-File Report*, U.S. Geological
546   Survey, 99-50

547 Bustin, R. M., & Chonchawalit, A. (1995). Formation and tectonic evolution of the pattani basin, gulf of thailand.
548   *International Geology Review*, 37(10), 866–892. https://doi.org/10.1080/00206819509465431

549 Daines, S. R. (1985). Structural History of the W Natuna Basin and the Tectonic Evolution of the Sunda Region, *14th*
550   *Annual Convention Proceedings (Volume 1)*, 39-61

551 Darmadi, Y., Willis, B. J., & Dorobek, S. L. (2007). Three-dimensional seismic architecture of fluvial sequences on the
552   low-gradient sunda shelf, offshore indonesia. *Journal of Sedimentary Research*, 77(3), 225–238.
553   https://doi.org/10.2110/jsr.2007.024

554 Doust, H. (2017). Petroleum systems in southeast asian tertiary basins. *Bulletin of the Geological Society of Malaysia*,
555   *64*(1), 1–16. https://doi.org/10.7186/bgsm64201701

556 Doust, H., & Sumner, H. S. (2007). Petroleum systems in rift basins – a collective approach in Southeast Asian
557   basins. *Petroleum Geoscience*, 13(2), 127–144. https://doi.org/10.1144/1354-079307-746

558 Du Bois, E. P. (1985). Review of principal hydrocarbon-bearing basins around the South China Sea. *Bulletin of the*
559   *Geological Society of Malaysia*, *18*, 167–209. https://doi.org/10.7186/bgsm18198508

560 Fyhn, M. B. W., Boldreel, L. O., & Nielsen, L. H. (2010). Escape tectonism in the Gulf of Thailand: Paleogene left-lateral
561   pull-apart rifting in the Vietnamese part of the Malay Basin. *Tectonophysics*, 483(3–4), 365–376.
562   https://doi.org/10.1016/j.tecto.2009.11.004

563 GEBCO Compilation Group. (2023). GEBCO 2023 Grid. https://doi.org/10.5285/F98B053B-0CBC-6C23-E053-
564   6C86ABC0AF7B

565 Ghosh, D., Halim, M. F. A., Brewer, M., Viratno, B., & Darman, N. (2010). Geophysical issues and challenges in Malay
566   and adjacent basins from an E & P perspective. The Leading Edge, 29(4), 436–449.
567   https://doi.org/10.1190/1.3378307

568 Ginger, D. C., Ardjakusumah, W. O., Hedley, R. J. & Pothecary, J. (1993). Inversion history of the West Natuna Basin:
569   Examples from the Cumi-Cumi PSC. *Proceedings Indonesian Petroleum Association: 22nd Annual Convention*,
570   635-658

571 Hasbollah, D. Z. A., Junin, R., Taib, A. M., & Mazlan, A. N. (2020). Basin evaluation of co2 geological storage potential
572   in malay basin, malaysia. In P. Duc Long & N. T. Dung (Eds.), *Geotechnics for Sustainable Infrastructure*
573   *Development* (Vol. 62, pp. 1405–1410). Springer Singapore. https://doi.org/10.1007/978-981-15-2184-3_184

574 Hall, R., & Morley, C. K. (2004). Sundaland basins. In P. Clift, W. Kuhnt, P. Wang, & D. Hayes (Eds.), *Geophysical*
575   *Monograph Series* (Vol. 149, pp. 55–85). American Geophysical Union. https://doi.org/10.1029/149GM04

576 Hall, R., Clements, B., & Smyth, H. R. (2009). Sundaland: Basement character, structure and plate tectonic
577   develoment. *Proc. Indon Petrol. Assoc., 33rd Ann. Conv*. Thirty-Third Annual Convention.
578   https://doi.org/10.29118/IPA.2374.09.G.134

579 Hou, J., Takahashi, T., Katoh, A., Jaroonsitha, S., Chumsena, K. P., & Nakayama, K. (2008). Application of seismic
580   attributes and neural network for sand probability prediction—A case study in the North Malay Basin.
581   *Bulletin of the Geological Society of Malaysia*, 54, 115–121. https://doi.org/10.7186/bgsm54200818

582 Jirin, S., Mohamed, M., & Hasan, S. S. (2013). Transgressive-regressive cycles in the malay basin: New insights. *IPTC*.
583   https://doi.org/10.2523/IPTC-16838-Abstract

584 Jumari, N. I., Mohaman, H. & Ahman, N. (2011). Seismic Facies Analysis of Group L and M Reservoirs Southeast of
585   Malay Basin. *Warta Geologi (Newsletter of the Geological Society of Malaysia)*, 37(1), 55

586 Kessler, F. L., Jong, J., & Madon, M. (2021). Sedimentary record of paleogene sequences in the penyu and malay
587   basins, offshore peninsular malaysia. *Berita Sedimentologi*, 46(1), 6–20.
588   https://doi.org/10.51835/bsed.2020.46.1.57

589 Kuang, K. S. (1988). Structural history of the Malay Basin, a classical Tertiary wrench basin. *Warta Geologi (Newsletter*
590   *of the Geological Society of Malaysia)*, 14(6)

591 Liew, K. K. (1994). Structural development at the west-central margin of the Malay Basin. *Bulletin of the Geological*
592   *Society of Malaysia*, 36, 67-80

593 Liew, K. K. (1997). Structural analysis of the Malay Basin. *Bulletin of the Geological Society of Malaysia*, 40, 157-176.
594   https://doi.org/10.7186/bgsm40199712

595 Lunt, P. (2021). A reappraisal of the cenozoic stratigraphy of the malay and west natuna basins. *Journal of Asian Earth*
596   *Sciences*: X, 5, 100044. https://doi.org/10.1016/j.jaesx.2020.100044

597 Madon, M. (1994). Depositional and diagenetic histories of reservoir sandstones in the Jerneh field, central Malay
598   Basin. *Bulletin of the Geological Society of Malaysia*, 36, 31-53.

599 Madon, M. (1997). The kinematics of extension and inversion in the Malay Basin, offshore Peninsular Malaysia.
600   *Bulletin of the Geological Society of Malaysia*, 41, 127–138. https://doi.org/10.7186/bgsm41199711

601 Madon, M. (2007). Overpressure development in rift basins: An example from the Malay Basin, offshore Peninsular
602   Malaysia. *Petroleum Geoscience*, 13(2), 169–180. https://doi.org/10.1144/1354-079307-744

603 Madon, M. (2011). Transgressive-Regressive Cycles in the Malay Basin: the Interplay of Tectonics and Sea Level
604   Changes in a Silled Basin, *PGCE 2011*. https://doi.org/10.3997/2214-4609-pdb.251.49

605 Madon, M. (2021). Five decades of petroleum exploration and discovery in the malay basin (1968-2018) and
606   remaining potential. *Bulletin of the Geological Society Of Malaysia*, *72*, 63–88.
607   https://doi.org/10.7186/bgsm72202106

608 Madon, M. & Watts. (1998). Gravity anomalies, subsidence history and the tectonic evolution of the Malay and Penyu
609   Basins (Offshore peninsular malaysia). *Basin Research*, 10(4), 375–392. https://doi.org/10.1046/j.1365-
610   2117.1998.00074.x

611 Madon, M., Abolins, P., Hoesni, M J., & Ahmad, B. (1999a). 'Malay Basin'. *The Petroleum Geology and Resources of*
612   *Malaysia*, Petronas. Kuala Lumpur, 173-217

613 Madon, M., Karim, R B A., & Fatt, R W H., (1999b). 'Tertiary Stratigraphy and Correlation Schemes. *The Petroleum*
614   *Geology and Resources of Malaysia*, Petronas. Kuala Lumpur, 115-137

615 Madon, M., Yang, J.-S., Abolins, P., Abu Hassan, R., M. Yakzan, A., & Zainal, S. B. (2006). Petroleum systems of the
616   northern malay basin. *Bulletin of the Geological Society of Malaysia*, 49, 125–134.
617   https://doi.org/10.7186/bgsm49200620

618 Madon, M., Jong, J., Kessler, F. L., Murphy, C., Your, L., A Hamid, M., & M Sharef, N. (2019). Overview of the structural
619   framework and hydrocarbon plays in the Penyu Basin, offshore Peninsular Malaysia. *Bulletin of the Geological*
620   *Society of Malaysia*, *68*, 1–23. https://doi.org/10.7186/bgsm68201901

621 Madon, M., Jong, J., Kessler, F. L., Damanhuri, M. H., & Amin, M. K. A. (2020). Pre-tertiary basement subcrops
622   beneath the malay and penyu basins, offshore peninsular malaysia: Their recognition and hydrocarbon
623   potential. *Bulletin of the Geological Society Of Malaysia*, *70*(1), 163–193.
624   https://doi.org/10.7186/bgsm70202014

625 Mansor, M. Y., Rahman, A. H. A., Menier, D., & Pubellier, M. (2014). Structural evolution of Malay Basin, its link to
626   Sunda Block tectonics. *Marine and Petroleum Geology*, 58, 736–748.
627   https://doi.org/10.1016/j.marpetgeo.2014.05.003

628 Matthews, S. J., Fraser, A. J., Lowe, S., Todd, S. P., & Peel, F. J. (1997). Structure, stratigraphy and petroleum geology of
629   the se nam con son basin, offshore vietnam. Geological Society, London, Special Publications, 126(1), 89–106.
630   https://doi.org/10.1144/GSL.SP.1997.126.01.07

631 McGrath, S. M., Clemens, S. C., & Huang, Y. (2023). Pleistocene Sunda Shelf submersion-exposure cycles initiate
632   vegetation Walker Circulation feedback. *Geology*. https://doi.org/10.1130/G51412.1

633 Metcalfe, I. (2009). Late palaeozoic and mesozoic tectonic and palaeogeographical evolution of se asia. *Geological*
634   *Society, London, Special Publications*, 315(1), 7–23. https://doi.org/10.1144/SP315.2

635 Metcalfe, I. (2011). Tectonic framework and Phanerozoic evolution of Sundaland. *Gondwana Research*, 19(1), 3–21.
636   https://doi.org/10.1016/j.gr.2010.02.016

637 Metcalfe, I. (2017). Tectonic evolution of Sundaland. *Bulletin of the Geological Society of Malaysia*, *63*, 27–60.
638   https://doi.org/10.7186/bgsm63201702

639 Miall, A.D. (2002). Architecture and sequence stratigraphy of Pleistocene fluvial systems in the Malay Basin, based on
640   seismic time-slice analysis. *AAPG Bulletin*, 86. https://doi.org/10.1306/61EEDC56-173E-11D7-
641   8645000102C1865D

642 Molnar, P., & Tapponnier, P. (1975). Cenozoic tectonics of asia: Effects of a continental collision: features of recent
643   continental tectonics in asia can be interpreted as results of the india-eurasia collision. *Science*, 189(4201),
644   419–426. https://doi.org/10.1126/science.189.4201.419

645 Morley, C. K. (2001). Combined escape tectonics and subduction rollback–back arc extension: A model for the
646   evolution of Tertiary rift basins in Thailand, Malaysia and Laos. *Journal of the Geological Society*, 158(3), 461–
647   474. https://doi.org/10.1144/jgs.158.3.461

648 Morley, C. K. (2002). A tectonic model for the Tertiary evolution of strike–slip faults and rift basins in SE
649   Asia. *Tectonophysics*, 347(4), 189–215. https://doi.org/10.1016/S0040-1951(02)00061-6

650 Morley, C. K. (2012). Late cretaceous–early palaeogene tectonic development of se asia. *Earth-Science
651   Reviews*, 115(1–2), 37–75. https://doi.org/10.1016/j.earscirev.2012.08.002

652 Morley, C. K. (2016). Major unconformities/termination of extension events and associated surfaces in the South
653   China Seas: Review and implications for tectonic development. *Journal of Asian Earth Sciences*, 120, 62–86.
654   https://doi.org/10.1016/j.jseaes.2016.01.013

655 Morley, R. J., Morley, H. P. & Restrepo-Pace, P. (2003). Unravelling the tectonically controlled stratigraphy of the West
656   Natuna Basin by means of palaeo-derived mid Tertiary climate changes. *Proceedings, Indonesian Petroleum
657   Association: 29th Annual Convention & Exhibition, October 2003*

658 Murray, M. R., & Dorobek, S. L. (2004). Sediment supply, tectonic subsidence, and basin-filling patterns across the
659   southwestern South China Sea during Pliocene to recent time. In P. Clift, W. Kuhnt, P. Wang, & D. Hayes
660   (Eds.), *Geophysical Monograph Series* (Vol. 149, pp. 235–254). American Geophysical Union.
661   https://doi.org/10.1029/149GM13

662 Nayak, S., Masoudi, R., Tarang Patrick Panting, A., B M Diah, M. A., B Roslan, M. R., B M Amin, M. F., R Iyer, S.,
663   Aarssen, B. V., Fun, S., & Mishra, S. (2023). Insights on the origin and distribution of co2 in malay basin,
664   offshore peninsular malaysia: A petroleum system modelling approach, IPTC-22832-EA.
665   https://doi.org/10.2523/IPTC-22832-EA

666 Ng, T S. (1987). Trap styles of the tenggol arch and the southern part of the malay basin. Bulletin of the Geological
667   Society of Malaysia, 21, 177–193. https://doi.org/10.7186/bgsm21198710.

668 Ngah, K., Madon, M., & Tjia, H. D. (1996). Role of pre-Tertiary fractures in formation and development of the Malay
669   and Penyu basins. *Geological Society, London, Special Publications*, 106(1), 281–289.
670   https://doi.org/10.1144/GSL.SP.1996.106.01.18

671 Petersen, H. I., Mathiesen, A., Fyhn, M. B. W., Dau, N. T., Bojesen-Koefoed, J. A., Nielsen, L. H., & Nytoft, H. P. (2011).
672   Modeling of petroleum generation in the Vietnamese part of the Malay Basin using measured kinetics. AAPG
673   Bulletin, 95(4), 509–536. https://doi.org/10.1306/09271009171

674 Pubellier, M., & Morley, C. K. (2014). The basins of Sundaland (Se asia): Evolution and boundary conditions. *Marine
675   and Petroleum Geology*, 58, 555–578. https://doi.org/10.1016/j.marpetgeo.2013.11.019

676 Ramli, M.D. (1988). Stratigraphy and palaeofacies development of carigali's operating areas in the malay basin, south
677   china sea. *Bulletin of the Geological Society of Malaysia*, *22*, 153–187.
678   https://doi.org/10.7186/bgsm22198808

679 Rice-Oxley, E., & Abu-Bakar, A. (2022). Historical and emerging super basins of Southeast Asia. *AAPG Bulletin*, 106(3),
680   633–653. https://doi.org/10.1306/09152121048

Rosly, S. F. M., Abdullah, M. S., Bukhari, M. K. A. M., Tazarudin, N., Nawawi, H. A. B. M., Pendkar, N., Panting, A. T. P., Zhou, J., & Torres, J. A. P. (2019). M-70 sand: Realizing the group m hidden opportunity in malay basin. *APGCE 2019*, 1–5. https://doi.org/10.3997/2214-4609.201903410

Shing, C.Y. (1992). Petrographic and diagenetic studies of the reservoir sandstone of the Malay Basin. *Bulletin of the Geological Society of Malaysia*, *32*, 261–283. https://doi.org/10.7186/bgsm32199216

Straume, E. O., Gaina, C., Medvedev, S., Hochmuth, K., Gohl, K., Whittaker, J. M., Abdul Fattah, R., Doornenbal, J. C., & Hopper, J. R. (2019). Globsed: Updated total sediment thickness in the world's oceans. *Geochemistry, Geophysics, Geosystems*, 20(4), 1756–1772. https://doi.org/10.1029/2018GC008115

Tapponnier, P., Peltzer, G., Le Dain, A. Y., Armijo, R., & Cobbold, P. (1982). Propagating extrusion tectonics in Asia: New insights from simple experiments with plasticine. *Geology*, 10(12), 611. https://doi.org/10.1130/0091-7613(1982)10<611:PETIAN>2.0.CO;2

Thye, Y. K. (1996). Sequence stratigraphy of the Group J, Tapis Field, Malay Basin, *Warta Geologi (Newsletter of the Geological Society of Malaysia)*, 22(6), 421-422

Tingay, M. R., Morley, C., Laird, A. P., Limpornpipat, O., Krisadasima, K., Pabchanda, S., & Macintyre, H. (2011). Overpressures in the northern malay basin: Part 1 - origin and distribution. All Days, IPTC-15345-MS. https://doi.org/10.2523/IPTC-15345-MS

Tingay, M. R. P., Morley, C. K., Laird, A., Limpornpipat, O., Krisadasima, K., Pabchanda, S., & Macintyre, H. R. (2013). Evidence for overpressure generation by kerogen-to-gas maturation in the northern Malay Basin. *AAPG Bulletin*, 97(4), 639–672. https://doi.org/10.1306/09041212032

Tjia, H.D. (1994). Inversion tectonics in the Malay Basin: evidence and timing of events. *Bulletin of the Geological Society of Malaysia*, 36, 119–126.

Tjia, H.D. (1998). Origin and Tectonic Development of Malay-Penyu-West Natuna Basins. *Bulletin of the Geological Society of Malaysia*, 42, 147–60. https://doi.org/10.7186/bgsm42199813.

Tjia, H. D. (2014). Wrench-Slip Reversals and Structural Inversions: Cenozoic Slide-Rule Tectonics in Sundaland. *Indonesian Journal on Geoscience*, 1(1), 35-52

Tjia, H. D., & Liew, K. K. (1996). Changes in tectonic stress field in northern Sunda Shelf basins. *Geological Society, London, Special Publications*, *106*(1), 291–306. https://doi.org/10.1144/GSL.SP.1996.106.01.19

Twarog, M. R., Culver, S. J., Mallinson, D. J., Leorri, E., Donovan, B., Harrison, E. I., Hindes, H., Reed, D., Horsman, E., Shazili, N. A. M., & Parham, P. R. (2021). Depositional environments and sequence stratigraphy of post-last glacial maximum incised valley-fill, Malay Basin, northern Sunda Shelf. *Marine Geology*, 436, 106457. https://doi.org/10.1016/j.margeo.2021.106457

Vincelette, R. R., Beaumont, E. A., & Foster, N. H. (1999). Classification of exploration traps. In E. A. Beaumont & N. H. Foster, Exploring for Oil and Gas Traps. American Association of Petroleum Geologists. https://doi.org/10.1306/TrHbk624C2

Westerhold, T., Marwan, N., Drury, A. J., Liebrand, D., Agnini, C., Anagnostou, E., Barnet, J. S. K., Bohaty, S. M., De Vleeschouwer, D., Florindo, F., Frederichs, T., Hodell, D. A., Holbourn, A. E., Kroon, D., Lauretano, V., Littler, K., Lourens, L. J., Lyle, M., Pälike, H., … Zachos, J. C. (2020). An astronomically dated record of Earth's climate and its predictability over the last 66 million years. *Science*, 369(6509), 1383–1387. https://doi.org/10.1126/science.aba6853

Woolands, M. A. & Haw, D. (1976). Tertiary Stratigraphy and Sedimentation in the Gulf of Thailand. *Offshore South East Asia Conference, 1976*, 63-84

Yakzan, M. A., Harun, A., Md Nasib, B., & Morley, R. J. (1996). Integrated biostratigraphic zonation for the Malay Basin. *Bulletin of the Geological Society of Malaysia*, *39*, 157–184. https://doi.org/10.7186/bgsm39199615

Yusak, S. A. M. (2012). Sedimentological Characterization of Deeper Group M Reservoirs in Malay Basin. *Warta Geologi (Newsletter of the Geological Society of Malaysia)*, 38(2), 212